APPLICATION OF HIGH-RESOLUTION NMR SPECTROSCOPY IN METABOLIC STUDIES OF THE EYE

by

Øystein Risa

A thesis in partial fulfilment of the requirements for the degree Doktor Ingeniør

Trondheim, autumn 2004

Norwegian University of Science and Technology
Faculty of Natural Sciences and Technology
Department of Physics

NTNU

Acknowledgements

I would like to thank my supervisors Professor Anna Midelfart (Department of Neurosciences, NTNU, former professor II at the department of physics, NTNU) and Professor Jostein Krane (Department of Chemistry, NTNU) for giving me the opportunity to explore the exiting field of eye research and NMR spectroscopy. Thank you for all the support, good advices and guidance through these years. I would also like to thank my patient lab/office-partner Oddbjørn Sæther for always being there to discuss important technical and theoretical aspects.

Thanks to everybody at the MR-Centre and the Department of Biotechnology for being such nice and helpful people and creating a great work environment. Special thanks to engineer Trond Singstad, Dr. Scient. Henrik W. Antonsen, Cand. Scient. Odd Inge Optun, Dr. Ing. John Georg Seland, and Dr. Phil. Beathe Sitter for helping me out with practical NMR problems.

I would like to give head engineer Bjørg Ulsaker special thanks for being encouraging in pressured times and for giving me time to finish my thesis during my teaching work at the Department of Biotechnology, NTNU.

My thanks also go to the colleagues at St. Erik's Eye Hospital, Karolinska Institutet in Stockholm and at the Department of Eye Histochemistry and Pharmacology, Academy of Science of the Czech Republic, Prague for nice and fruitful collaboration during these years.

My gratitude and love to my wife Jenny and my little daughter Johanne. You have been more than patient to me, and given me unconditional love throughout all these years I have been working on my thesis. My love also goes to my parents, sisters, brother, and family in law who always are there for me.

This work has been financially supported by grants from Health and Rehabilitation, Norway.

Trondheim, 2004

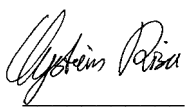

Øystein Risa

Summary

High-resolution NMR spectroscopy has, during the last two decades, had an increasing impact in biological and biochemical research. Rapid advances have led to improvements in sensitivity and dispersion of the spectra and have allowed more detailed assignment and monitoring of endogenous biochemical molecules. One of the latest implementations has been a technique known as high-resolution magic angle spinning (HR-MAS) NMR spectroscopy which has made it possible to obtain high-resolution proton spectra of intact tissue and cells. Simultaneous detection of a large number of metabolites by NMR spectroscopy has been successfully applied to investigate disordered metabolism for a numerous of diseases and toxic processes.

The objectives in the present work have been to evaluate different ^{1}H NMR spectroscopy protocols as analytical tools in eye research, and further use these protocols to extract and interpret information on metabolic changes in the eye induced by external pathological stimuli. Special focus has been paid to changes in the lens and the development of cataracts.

The ^{1}H NMR spectra of intact lenses and eye tissue extracts in present thesis showed an extensive picture of NMR detectable metabolites. In addition to the detailed analysis of extracts from cornea, lens and aqueous humour, this work has created a basis for implementation and interpretation of HR-MAS ^{1}H NMR spectroscopy on intact lens tissue.
Several significant changes in the metabolic content in cornea, aqueous humour, and lens after alkali-burns to the eye were detected, and showed how careful ^{1}H NMR spectroscopy analysis of tissue extracts provided new information (quantitative and qualitative) on the metabolic reaction pattern in the anterior eye segment in relation to eye alkali-burn injuries.

HR-MAS studies on lenses exposed *in vivo* to different ultraviolet-B doses did not reveal any dose-response relationship for the metabolic changes. However, significant concentration changes for most of the observed metabolites seven days post exposure demonstrated that close-to-threshold UVB radiation had great impact on the metabolites in the lens. Further time dependency studies of metabolic changes in rat lens after UVB radiation showed that significant changes in metabolite concentrations were subsequent to lens opacity development.
Long-term steroid treatment (36 days) seemed to have greater impact on the metabolic changes compared to the UVB-induced changes 24 hours after UVB radiation. Even though no obvious cataract was detected after the combined treatment of steroids and UVB radiation, significant changes were observed for several metabolites.

Contributions to the papers

The studies present in the papers of this thesis have been a collaboration between laboratories in Trondheim, (Norway), Stockholm, (Sweden) and Prague, (Czech Republic).

The extraction procedures, lactate assay, and all the experimental NMR work in paper I-III were carried out by Risa Ø. In paper IV detailed analyses and interpretations of the acquired NMR spectra were performed by Risa, Ø. and Sæther O. in cooperation.

The animal experiments on the rabbits in paper I and IV were performed by Čejková J and colleagues in Prague. The *in vivo* UVB exposure experiments on rats in paper II and III were done by the Söderberg group in Stockholm.

List of Appendix Papers

I. Risa Ø, Sæther O, Midelfart A, Krane J, Čejková J (2002) Analysis of immediate changes of water-soluble metabolites in alkali-burned rabbit cornea, aqueous humour and lens by high-resolution ^{1}H-NMR spectroscopy. Graefe's Arch Clin Exp Ophthalmol 240: 49-55

II. Risa Ø, Sæther O, Löfgren S, Söderberg PG, Krane J, Midelfart A (2004) Metabolic changes in rat lens after *in vivo* exposure to ultraviolet irradiation: measurements by high-resolution MAS ^{1}H NMR spectroscopy. Invest Ophthalmol Vis Sci 45: 1916-1921

III. Risa Ø, Sæther O, Kakar M, Mody V, Löfgren S, Söderberg PG, Krane J, Midelfart A (2004) Time dependency of metabolic changes in rat lens after *in vivo* UVB exposure analysed by HR-MAS ^{1}H NMR spectroscopy. Submitted to Exp Eye Res

IV. Sæther O, Risa Ø, Čejková J, Krane J, Midelfart A (2004) High-resolution magic angle spinning ^{1}H NMR spectroscopy of metabolic changes in rabbit lens after treatment with dexamethasone combined with UVB exposure. Accepted in Graefe's Arch Clin Exp Ophthalmol

Abbreviations

AH	Aqueous Humour
COSY	Correlated Spectroscopy
CPMG	Carr-Purcell-Meiboom-Gill (pulse sequence)
$_t$EDC	transformed Equivalent Diazepam Concentrations
FID	Free Induction Decay
GSH	Reduced glutathione
HR-MAS	High-Resolution Magic Angle Spinning
JRES	J-resolved (J = spin-spin coupling)
M/C	Methanol/Chloroform
NMR	Nuclear Magnetic Resonance
PCA	Perchloric Acid
ppm	Parts per million
T_1	Longitudinal relaxation
T_2	Transversal relaxation
TSP	Sodium-3'-trimethylsilylpropionate-2,2,3,3-d_4
UVR	Ultraviolet Radiation
1D	One-dimensional
2D	Two-dimensional
^{1}H	Proton nucleus
^{31}P	Phosphorus nucleus

Table of Contents

1. Background

1.1 The eye

The eye is a specialised organ for photoreception, the process by which light energy from the environment produces changes in photoreceptors in the retina, the rods and cones. Those wavelengths capable of stimulating the receptors of the human eye are between 400 and 700 nm (the visible spectrum). The changes in the photoreceptor cells result in nerve action potentials which are subsequently relayed to the optic nerve and then to the visual cortex in the brain, were the information is processed and appreciated as vision. The structures in the eye are based on these basic physiological processes. Some parts of the system are necessary for focusing and transmitting the light onto the retina, for example the cornea, lens and ciliary body (Fig. 1.1). The iris regulates the amount of light entering the eye. Other parts are necessary for nutrition and support of the eye tissue for example the aqueous humour (AH), the tear film and the choroid (a thin vascular coat between sclera and retina). The eye is a unique organ because it is relatively unprotected and is constantly exposed to radiation, atmospheric oxygen, environmental chemicals and physical abrasion. Each of these factors results in generation of reactive oxygen species that may contribute to ocular damage and disease. A good and healthy metabolism in the eye is necessary to maintain the vital functions [1].

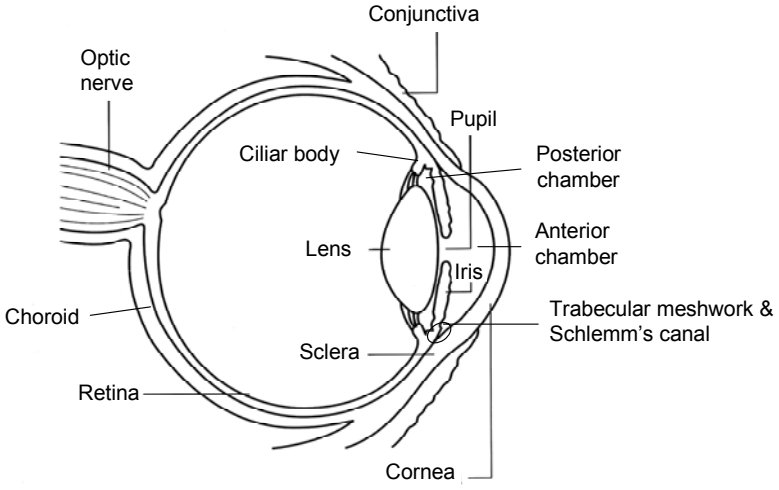

Figure 1.1 Anatomy diagram of the human eye showing the major components of the horizontal section.

Cornea

The cornea is transparent and is the main light refracting element in the eye, providing 2/3 of the eye's focusing power. The cornea is composed of five distinct anatomic layers; the outermost epithelial layer, the basal lamina underlying the epithelium, the stroma which comprises about 90 % of the thickness, the Descemet's membrane and the innermost endothelium. The major structural components are collagen and proteoglycans (12 – 15 % and 1 – 3 % of the wet weight respectively). In addition there are other noncollagenous structural proteins, soluble proteins, glycoproteins and lipids.
Being an avascular tissue, the nutritional needs of the cornea are met by the tear film (the source of the atmospheric oxygen) and the AH (the major source of glucose) [2].

The cornea's ability to transmit light is a function of how the cells and matrix components are organized within the tissue to minimise the refractive index disparity.
This regular arrangement is highly dependent on the state of hydration, metabolism and nutrition of the corneal stroma [2]. When the stroma swells it loses its transparency [3]. Thus maintaining the osmotic balance is essential for the cornea [4, 5].
Corneal epithelium is the major centre of oxidative metabolism. In addition it provides an essential function in protecting the cornea from damage by noxious and infectious agents [6]. The properties of the corneal epithelial surface are sustained by continuous renewal finely balanced between epithelial proliferation, differentiation and cell death. Studies of corneal wound healing, e.g. after alkali-burn damage [7, 8], have yielded useful information for the understanding of the maintenance of corneal epithelial functions.

Another important task for the cornea in general is to protect the underlying eye tissue from damaging ultraviolet radiation (UVR) [9]. Ultraviolet-C (UVC) rays at wavelengths over a range of 100 - 290 nm is completely absorbed by the cornea. Eighty per cent of exposed UVB rays at wavelengths over a range of 290 - 320 nm are absorbed in the cornea epithelium. Additionally, 34% of exposed UVA radiation over a range of 320 - 400 nm is absorbed in the cornea and the remainder passes through it [10].

Aqueous Humour

Aqueous humour (AH) is a transparent fluid located in the anterior and posterior chambers of the eye (Fig. 1.1). AH is secreted from the ciliary body/epithelium into the posterior chamber, and it is generally believed that the metabolic composition of AH is mostly regulated by active transport [11]. It then circulates through the pupil into the anterior chamber. The main portion of AH leaves the eye through the trabecular meshwork into Schlemm's canal. The remainder escapes through the sclera. In human eyes the rate of AH formation is about 2 – 3 μl/min [12]. AH supplies nutrients and oxygen to and removes metabolic wastes from the anterior intraocular tissues such as the cornea, lens and trabecular meshwork. It maintains intraocular pressure (IOP) for normal optical function of the eye, and facilitates the local immune response during inflammation and infection together with protection against oxidative damage [1].

The AH is composed predominantly of electrolytes and low molecular weight compounds with some protein. To *et al*. [11] have reported that among the most abundant metabolites are urea, glucose, lactate and ascorbate. However, other metabolites may also be present in relative high concentrations like inositols, citrate and some amino acids (paper I). The concentrations of several components differ significantly from plasma levels, for example the protein content of AH which is very low (about 1/500 of plasma) and ascorbate concentrations that reach levels 50 times higher than those in the blood plasma [11]. Ascorbate is considered to be an important antioxidant for instance in protecting the eyes against photo-oxidative damage [13, 14]. Unpublished studies from our laboratory have revealed a significant decrease in ascorbate in AH after moderate *in vivo* UVB irradiation of rabbit eyes [15]. It has also been suggested that the high ascorbate level in AH may protect cornea against ulceration and perforation following experimental alkali burns [16, 17]. Further roles of different metabolites in AH are discussed in paper I.

Lens

The lens plays an integral part in the focusing of light onto the retina. By changing its shape the focal power of the eye is changed, allowing an individual to focus on objects

at varying distances (accommodation). To perform its function the lens must be transparent, flexible and possess a relatively high refractive index.

The lens is a cellular, avascular organ surrounded by a strong and elastic collagenous capsule. Beneath the capsule the lens is made up predominantly of elongated fibre cells formed by the differentiation of epithelial cells that line the anterior surface of the lens. During differentiation, fibre cells lose their cytoplasmic organelles and begin to express lens-specific proteins known as crystallins. The high concentration of crystallins (up to 40% in the human lens nucleus and 50% in the rat lens nucleus) is responsible for the high refractive index in the lens, and the breakdown of organelles probably enhances the transparency in the central part of the lens. The disadvantage of not having organelles is that damage to these cells cannot always be repaired. Lens growth continues throughout the lifetime with new fibre cells being laid on top of existing fibre cells. The older primary fibre cells are compressed inward, forming a central "nuclear region" of the mature lens. Thus, the cells in the centre of the lens contain protein molecules that are as old as the individual. Maintenance of this architecture requires refined mechanisms not only for nourishment but also to control cell volume and protect against oxidative damage [1].

1.2 Alkali-burn injuries in the eye

Wide use of chemicals in the home and workplace makes toxic exposure, and thus the potential of injuries, unavoidable. In the U.S. alone ~ 22 500 cases of chemical eye burns were reported by the U.S. Consumer Protection Safety Commission in 1978 [18]. In Norway chemical injuries to the eyes seem to affect all age groups and both sexes, the most severe cases tend to occur to men during their working years, and alkali chemicals are the most frequent cause of injury [19]. Some common caustic solutions are calcium hydroxide (lime and cement) and sodium hydroxide (cleaners) in industry and ammonium hydroxide (fertilisers) in farming.

Alkali burns to the eye are among the most disastrous of ocular injuries and are usually more destructive than acid burns. Alkali damages the eye by increasing the hydroxyl ion concentration beyond the limits of protein stability. This leads to saponification of the lipid cellular membranes and allows the alkali agents to rapidly penetrate the ocular

tissue. Unlike acids, which tend to cause self-limiting injury, alkalis promote their own penetration of the eye [20].

Characteristically, severe alkali-burns result in blinding corneal opacification and limbal ischemia which inhibits wound healing. The ciliary body may also suffer from ischemic damage and under such conditions nutrient metabolites might be deficient in the anterior segment of the eye [21].
One of the most serious complications after alkali burn to the eye is ulceration, which can occur within weeks of the initial injury and progress to corneal perforation, commonly causing irreversible blindness. To prevent ulceration, a multitude of medications are used to promote collagen synthesis, inhibit the enzyme collagenase, and enhance epithelization [22]. Extensive studies on wound healing [7] and enzymatic changes after alkali-burn [23, 24] have lead to a better insight into the different repair mechanisms and the development of corneal ulceration. However, basic knowledge of the immediate biochemical and physiological changes in the anterior segment of the eye after severe burning is also important for developing rational approaches to acute treatment and therapeutic regiments. In Paper I in the present thesis, the immediate alkali-induced changes of the water-soluble metabolites in cornea, AH and lens were investigated.

1.3 Cataracts

Cataracts are a leading cause of visual impairment and blindness, and an ever-increasing health problem with the aging of the world population. In US approximately 1.35 million cataract surgeries are performed annually at a cost of more than $3 billion. In Norway over 45.000 cataract surgeries are preformed annually in public hospitals. The prevalence of cataracts approximately doubles with each decade after the age of 30 [25].

Since the beginning of the 20th century, research on chemical composition and metabolism of the lens has been conducted to better understand the existence and maintenance of lens transparency [26]. However, the mechanisms that initiate the cataract development still remain unclear. Cataracts are considered to be a multifactoral

disease [25] and among possible risk factors are: metabolic disorders, toxic agents, trauma, UVR, nutritional deficiencies, smoking, alcohol and hereditary factors.

A cataract in its broadest definition is opacity in the lens that disturbs vision. The opacity might occur everywhere in the lens, but the common types are cortical, nuclear, and sub-capsular cataract. In the normal lens, densely packed crystallines exist in a highly ordered arrangement to maintain lens transparency. Any abruption or irregular changes in the protein arrangement may result in loss of transparency contributing to the development of a cataract. Irregular changes might be protein aggregation, membrane degeneration, fluctuations in protein distribution or phase separation, all resulting in local changes of refractive index. For further reading, the great variety of metabolic insults that can cause cataracts has been described in detail by Harding and Crabbe [27].

UVR and cataracts

The investigation of UVR as a risk factor for cataracts has received considerable attention the last decade. Depletion of the stratospheric ozone will lead to UV exposure of higher intensity [28], and even if the risk for cataract development from UVR was relative low, the effect could be significant because nearly everyone is exposed. Several epidemiologic research reports have indicated an association between UVR and cataract formation [29-31]. UVR may cause temporary or permanent impairment to the lens depending on the dose. The wavelength range shown to be most harmful to the lens is UVB light in the region 300 to 305 nm [32, 33]. Therefore, to study the recovery pattern after UVR damage it is important to establish threshold UVR doses [33, 34], where doses below threshold only cause temporary cataractogenesis.

There are multiple mechanisms through which UVR damages the lens and contributes to cataract formation. Absorbed UVR photons excite lens molecules, creating free radicals and other reactive oxygen species (e.g. $^1O_2$, $O_2^{-}\cdot$, H_2O_2 and $^{\cdot}OH$), which increase the oxidative stress on the lens. This might induce damage to the DNA, proteins and lipids. Proteins are one of the major targets for photo-oxidation [35]. The major chromophoric amino acid present in proteins is tryptophan. However other amino acids like tyrosine, phenylalanine, histidine, cysteine and cystine also contribute to the

absorption of UV light [36]. The generated excited sites of the amino acids in the proteins may react with other proteins and form cross-links and aggregates. The anterior part of the eye contains several metabolites like GSH [37], taurine [38] and ascorbate [39] that function as antioxidants. The lens also contains UV scavengers that absorb damaging light [40].

Inhibition of enzymes [41, 42] and membrane protein damage [43] are also possible outcomes of direct protein UV absorbtion.

The DNA damage affects the lens cell differentiation and protein synthesis.

Lipid peroxidation and the inhibition of oxidative enzymes alter membrane functions and cell metabolism that further lead to osmotic stress, hypotonic conditions, cellular edema, and may in the end lead to cell death [44, 45]. In such cases osmolytes play a crucial role in protecting the lens from permanent damage. A sketch of possible pathways for cellular damage in the lens induced by UVR is shown in Fig. 1.2.

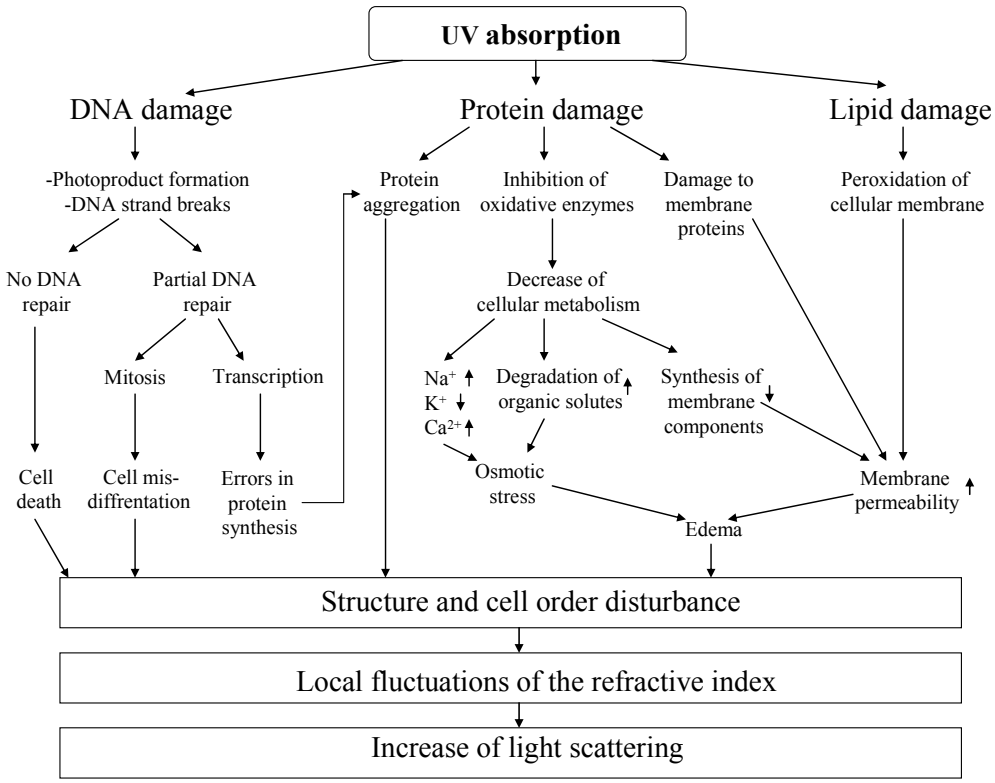

Figure 1.2 Possible pathways for cellular damage in the lens induced by UVR (↑ increase ↓ decrease). Figure is adapted from Michael R. thesis, 2000 [46].

Despite the impressive research effort, the metabolic changes involved in these processes are by no means clear. Particularly, reports on UVR induced effects on the endogenous metabolites are scarce. Screening the multiparametric metabolic response in the lens after UVR might provide better insight for interpretation of the biochemical events described in Fig. 1.2.

So far there is no initiating factor that explains all cataract types, but there might be metabolic responses that occur in all cataracts, after the initiating event. Most of the potential damage mechanisms described in Fig. 1.2 are not specific for UV cataract alone. Many of the endogenous metabolites are involved in key cellular pathways or have independent protective roles. Therefore, investigation of the metabolic changes initiated by UVR may also contribute to our general understanding of cataract development.

1.4 NMR spectroscopy

The first experiments and discoveries regarding nuclear magnetic resonance (NMR) were executed by Felix Bloch [47] and Edward Purcell [48] in 1946 and for this work they received the Nobel Prize in physics in 1952. Since then NMR has been a valuable tool for organic structure determination. NMR spectroscopy is based on the magnetic properties of nuclei (magnetic moment (μ) and nuclear spin (I)). Magnetic resonance arises from the interaction of certain nuclei with nuclear spin ($I \neq 0$) and radio frequent (rf) energy in the presence of a strong magnetic field. Each chemically distinct atomic nucleus gives detectable signals which are interpreted in terms of frequencies (chemical shifts, δ). The appearance of a specific peak depends on the molecular environments of the originating nuclei. The intensities of the NMR resonances are directly related to the number of nuclei contributing to them, and are the basis for calculation of the concentrations of substances in the sample. Isotopes like ^{1}H, ^{13}C and ^{31}P are by far the most used isotopes in NMR spectroscopy on biological materials, but a number of other molecules have also been studied, including ^{15}N, ^{19}F and ^{23}Na.

Many pieces of structural information can be obtained by NMR spectroscopy, including the spin-spin coupling pattern (multiplicity) and coupling constants (J) which are

important parameters in peak assignment of spectra. Nuclear Overhauser Enhancement (NOE) that is often used to measure intramolecular distances, and the two characteristic relaxation properties describing the reversion of nuclei to equilibrium: longitudinal (T_1) and transversal (T_2) relaxation. For a more detailed description of the physics that forms the basis of NMR spectroscopy, several introductory books are available [49, 50].

Magic Angle Spinning (MAS)

The observation of metabolites within intact tissue by ^{1}H NMR spectroscopy is confounded by a number of physical factors which broaden spectral resonances, including dipolar couplings, chemical shift anisotropy, and bulk magnetic susceptibility differences. Many of these line broadening factors are reduced by spinning the sample at the "magic" angle θ = 54.7° (angle between the spinning axis and the magnetic field B_0). Both dipolar couplings and chemical shift anisotropy are scaled by the angle dependency ($3\cos^2\theta - 1$), which are averaged to zero at 54.7°. For the line narrowing to be successful the spinning-rate must be comparable with the NMR linewidth of the material in static conditions, and is typically ~ 4 - 6 kHz for intact biological tissue [51]. Lower spin-rates may lead to unwanted spin sideband within the region of interest.

The effect of MAS on the dipolar couplings and chemical shift anisotropy are illustrated to the left in Fig. 1.3. The interaction vectors ($\mathbf{r}_{ax}$) between each pair of nuclei are averaged around magic angle (θ) by spinning the rotor. Within the past few years, the development of high-resolution MAS ^{1}H NMR in combination with line narrowing multipulse techniques have had substantial impact on the analysis of small intact tissue samples [52-56]. The MAS rotor volume may vary from about ~10µl to 100µl. Rotors with volume size 92µl (A) and 50µl (B) are shown to the right in Fig. 1.3

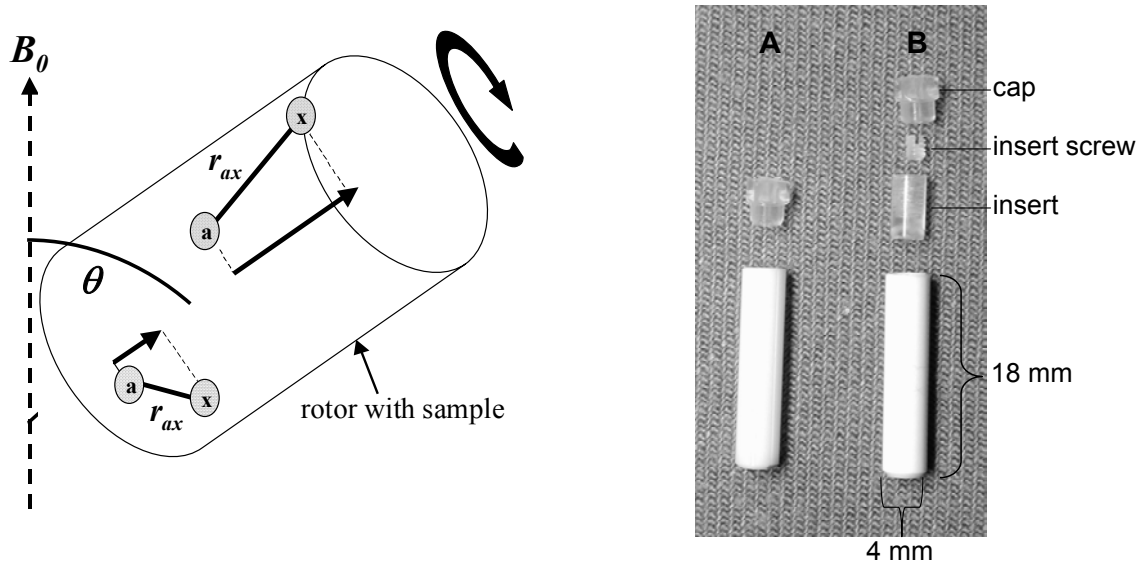

Figure 1.3 To the left: effect of MAS on the dipolar couplings and chemical shift anisotropy. Interaction vectors ($\mathbf{r}_{ax}$) between the nuclei (a and x) are averaged around the magic angle (θ) by spinning the rotor. B_0 = direction of the magnetic field. To the right: picture of zirconia HR-MAS rotors without insert 92µl (A) and with insert 50µl (B).

1.5 NMR spectroscopy in ophthalmic research

The development of more advanced spectrometers in the 1970's established the applicability of NMR spectroscopy in metabolic studies of biological systems. Now, for almost three decades, high-resolution NMR spectroscopy has been utilized in metabolic eye research. The earliest high-resolution NMR studies of the eye done by Greiner and Glonek *et al*. used phosphorus-31 (^{31}P) NMR spectroscopy to investigate the principal organophosphates on extracts and intact lenses [57, 58] and corneas [59]. The same group also documented the organophosphate profile of AH and vitreous body extracts from porcine eyes [60]. By using ^{31}P NMR spectroscopy the metabolic response in cornea to soft [61] and hard [62] contact lenses was investigated. Corneal vitamin A deficiencies [63] and corneal epithelial wound healing [64] have been analysed. It was also possible to follow up metabolic changes in the lens during development of cold cataract [65], upon treatment with dexamethasone [66], after UV exposure [67], and to investigate phosphorylated sugars in maturing rat lenses [68, 69]. Since some of the ^{31}P

shifts of phosphorus containing metabolites are pH-dependent, intracellular pH values could be monitored non-invasively in cornea and lens [70].

In comparison to ^{31}P NMR spectroscopy, the greatest sensitivity possible in NMR studies of biological materials is offered by observation of protons. Proton has the highest sensitivity of any stable nucleus, with close to 100% natural abundance and is found in virtually all metabolites. This gives ^{1}H NMR spectroscopy a great potential as a more complete analytic tool for complex mixtures. However, the disadvantages of ^{1}H NMR spectroscopy have been the narrow chemical shift range (~ 10 ppm) combined with high abundance of metabolites, large signal from water which must be suppressed, and the potential broad resonances from lipids and proteins which have to be reduced or eliminated. Stronger homogenous magnetic fields, improved computers, more sophisticated pulse sequences (two-dimensional (2D) techniques), and development of advanced water suppression techniques have indeed made ^{1}H and combined ^{1}H and ^{13}C NMR spectroscopy an important tool for identification and quantification of metabolites in biofluids and tissue extracts. The first medical applications showing the utility of the ^{1}H NMR analysis of complex metabolite mixtures involved analysis of serum [71, 72] and urine [73, 74].

Based on these pioneer studies the first one-dimensional (1D) ^{1}H NMR analysis of the eye was performed on human AH [75] with a further more detailed 2D ^{1}H NMR analysis on rabbit AH by Gribbestad and Midelfart [76]. The metabolic profile based on ^{1}H NMR spectroscopy has also been monitored for several eye tissue extracts, for example rabbit cornea [77], lens [78], conjunctiva and iris ciliary body [79]. Combined studies of ^{1}H and ^{19}F NMR have been performed to investigate the penetration of topical applied dexamethasone and dexamethosone phosphate in AH [80], cornea, and lens [81], with following ^{1}H NMR studies of metabolic changes in rabbit lenses induced by long-term topical treatment of dexamethasone [82]. The last reported ^{1}H NMR work on eye tissue extracts was the analysis of immediate changes in alkali-burned rabbit cornea, AH, and lens (paper I).

Until recently only ^{31}P NMR has been used to study the intact cornea and lens. However during the last decade new developments (HR-MAS) have established ^{1}H NMR as a valuable tool for metabolic screening of intact tissues, and has been successfully applied

to investigate numerous mammalian tissues and diseased tissues such as liver [83], brain [84], breast cancer [53, 55], renal cortex and medulla [54], testicular tissue [85], kidney [52], and cervical cancer [86]. The present thesis has been focused on utilization of this progress in ^{1}H NMR spectroscopy, to investigate metabolites in intact lens tissue in conjunction with cataract formation. The development of cataracts is a complex process associated with noxious influences on a number of biological pathways. ^{1}H NMR provides simultaneous information on many different metabolites and may therefore be a powerful analytical tool for the understanding of cataractogenesis.

2. Aim of the studies

The main objective of the experimental work included in this project has been to use different ^{1}H NMR spectroscopy procedures as analytical tools in ophthalmic research to extract and interpret information on metabolic changes in the eye induced by external pathological stimuli. Special focus has been paid to changes in the lens and cataract development. The more specific aims of this study were to:

1. Utilize high-resolution ^{1}H NMR spectroscopy on eye tissue extracts to access information of the immediate metabolic changes in the anterior eye segment after alkali-burns.

2. Evaluate the potential of high-resolution HR-MAS spectroscopy to be used in study of intact eye tissue.

3. Use HR-MAS spectroscopy to investigate possible changes in endogenous metabolites of intact lens tissue induced by UVB radiation, and further evaluate how different UVB doses make an impact on the severity of these changes.

4. Monitor how UVB induced metabolic changes in the lens developed over time compared to the cataract development.

5. Investigate how long-term treatment with dexamethasone combined with subsequent UVB exposure affected the metabolism in the lens compared to UVB radiation alone.

3. Experimental Aspects

3.1 UVB irradiation and light scattering measurements

The UVB doses described in paper II-VI were defined as the radiation energy per unit area reaching the anterior surface of the cornea. The animals were irradiated *in vivo* and the exposure time varied from 10 minutes (paper IV) to 15 minutes (paper II & III). All animals were kept and treated according to the ARVO Statement for the Use of Animals in Ophthalmic and Vision Research. When irradiation is quantified certain quantities such as radiance (W/m^2) or dose (radiance × exposure time, $Ws/m^2 = J/m^2$) may be used to describe the amount of radiation.

The degree of cataract in paper II and III was quantified with an objective light-scatter-measuring technique developed by Söderberg [87] using a Light Dissemination Meter (schematic drawing published by Söderberg [87]). The light scattering of the lens was calibrated against the scatter readings from a commercial available lipid emulsion, Diazemuls (Kabi Vitrum, Sweden). Diazemuls is a licensed preparation of oil in water emulsion with diazepam dissolved in the oil phase. This allowed conversion from relative current readings of forward light scattering to absolute transformed Equivalent Diazepam Concentrations ($_t$EDC). A typical value for a normal rat lens is about 0.1 $_t$EDC and for a very opaque lens about 1.0 $_t$EDC. Measured intensities of forward light scattering compared with photographs of isolated rat lenses are illustrated by Michael *et al*. [88]. Pictures of representative rat lenses analysed in paper II are shown in Fig. 3.1. The light scattering results presented in paper II and III are the difference in $_t$EDC between control and exposed lenses.

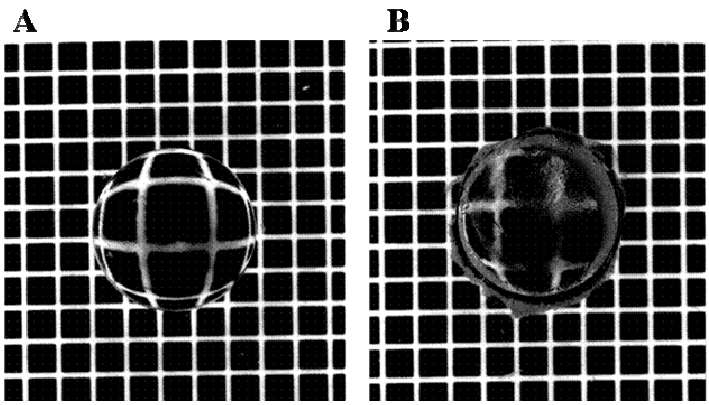

Figure 3.1 Picture of isolated control and exposed rat lenses one week after exposure to 5 kJ/m^2 UVB doses. Grid size 0.75 mm. Mean values for measured intensity of forward light scattering was 0.19 for the control (A) and 0.42 for the exposed (B) lens.

3.2 Comparison of extraction methods

For the extraction of water-soluble metabolites (e.g. amino acids and sugars) from biological tissue, perchloric acid (PCA) extraction has routinely been used in NMR studies [89, 90]. PCA extraction prevents enzymatic degradation during extraction while removing proteins and acidic macromolecules. PCA extraction has been widely used in NMR studies of water-soluble metabolites in the eye [57, 58, 77, 78, 91]. ^{1}H NMR studies on brain extracts by Le-Belle *et al.* [92] have shown that methanol/chloroform (M/C) extraction revealed significant higher yields of water-soluble metabolites compared to PCA extraction. In this project the two extraction methods were tested on water-soluble metabolites in rat lens tissue and compared by ^{1}H NMR spectroscopy.

Experimental description of the extraction methods

Frozen lenses excised from nine Sprague Dawley rats were pulverised with a porcelain mortar and pestle chilled in liquid nitrogen. The PCA extraction procedure was described in detail in paper I.

The M/C extraction of the lenses was performed as described by Le-Belle *et al* [92]. For the M/C extraction 50µl 0.9% NaCl solution was added to the pulverized tissue, and then the tissue-solvent mixture was transferred to a centrifuge tube. 360µl methanol/chloroform in a ratio of 2:1 was then added to the centrifuge tube and the tissue-solvent mixture was sonicated for 15 min. After sonication, 200µl

chloroform/distilled water in a ratio 1:1 was added to the M/C tissue mixture and the sample was centrifuged at ~ 3000 g for 15 minutes. The supernatant (methanol and water) was collected for analysis of water-soluble metabolites.

Extractions were done with pools of three lenses to get a proper signal-to-noise ratio. To remove water the PCA extracts were freeze dried and M/C extracts were dried at room temperature under a steam of nitrogen gas. ^{1}H NMR spectra were recorded at 25°C using a 90° pulse, acquisition time of 3.0 s and repetition delay of 5.0 s. TSP (sodium-3'-trimethylsilylpropionate-2,2,3,3-d_4) was used as an internal quantitative standard. The results are given in Fig. 3.2.

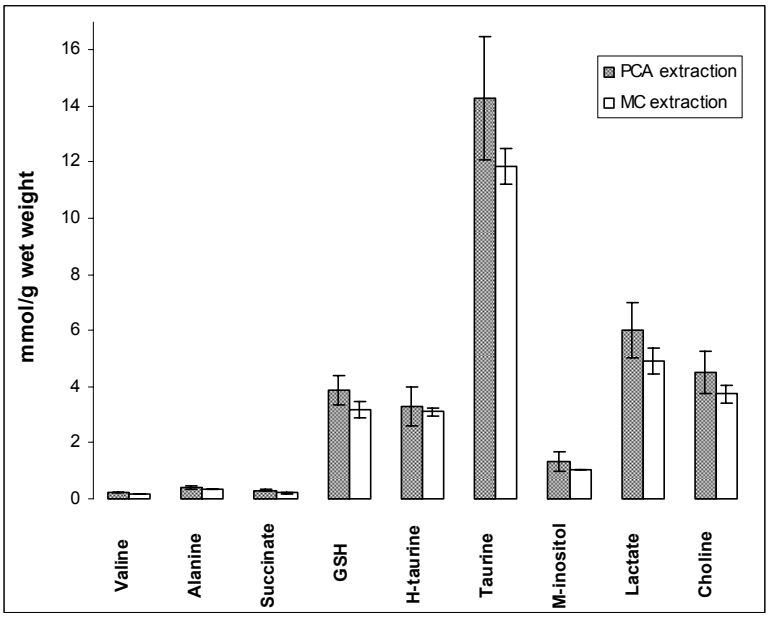

Figure 3.2 Concentration of metabolites in normal rat lens from PCA extracts (n = 3) and M/C extracts (n = 3). TSP was used as internal standard for concentration measurements. The bars represent the SD.

In contradiction to the findings by Le-Belle *et al.* [92], PCA extraction seemed to give the highest yield in lens tissue extracts (Fig. 3.2). From the analysed spectra, PCA extraction also showed a slightly lower background of residual macromolecules compared to the M/C method. Proton NMR studies on different protocols of lymphocyte extracts also suggested PCA as the optimum procedure for analysing water-soluble metabolites [93]. In the present study focusing on water-soluble metabolites in the eye tissue, PCA extraction seemed to be the best choice. However, M/C extraction enables profile analysis of both aqueous metabolites and lipids. ^{31}P NMR studies of M/C on extracts of human and animal lenses have been done to

investigate the lipid composition [94, 95], but to my knowledge high-resolution ^{1}H NMR studies on lipid composition of eye tissue have not been reported in literature.

3.3 Absolute quantification of metabolites in NMR spectroscopy

The fact that the area of a resonance peak is proportional to the number of nuclei, gives rise to an extensive use of quantitative measurement by NMR spectroscopists. Proton is the most sensitive nucleus to be observed by NMR due to the favourable gyromagnetic ratio and the natural abundance of 99.98%. The minimum concentration that can be detected depends upon many factors such as field strength and homogeneity, sample size, data collection times, and the acquisition parameters. The detection limit for ^{1}H at the field strength of 11.7 Tesla (500 MHz) is between 0.05 and 0.1mM depending on the metabolite observed. Thus the absence of a metabolite in an NMR spectrum only sets an upper limit on its concentration and cannot be taken as evidence of missing metabolites.

As compared to enzymatic and chromatographic methods, an inherent advantage of NMR spectroscopy is the simultaneous detection of a large number of metabolites without need for purification and derivatisation of individual metabolites prior to the analysis. Better probes, stronger magnetic fields and more sophisticated equipment are also continuously challenging the detection limits. However, NMR spectroscopy will always be less sensitive than chromatography methods like HPCL and GC/MS.

The absolute concentration of metabolites present in an extract can either be quantified by adding an internal standard, or by applying an external standard in a capillary of known concentration and volume. Alternatively the concentration of one of the endogenous metabolites can be assayed using other biochemical methods. Tofts and Wray have published a detailed description of the necessary assessments for quantification of metabolites by NMR spectroscopy [96].

T_1 measurements of metabolites from PCA lens extract

For a specific NMR experiment attention must be paid to the acquisition parameters under which the spectrum is obtained. (i) The acquisition time must be long enough to collect all of the free induction decay (FID) otherwise there will be truncation artefacts in the spectra and loss in signal-to-noise ratio. (ii) The pulses should be short

enough to cover the range of the chemical shifts present in the spectrum, otherwise the peaks near the edge of the spectrum will experience an area reduction. The pulse duration should not exceed 1/(4 × spectral width) which is 50 μs for a 5 kHz offset. Normally this is not a problem in ^{1}H NMR spectroscopy, but can occur in nuclei with large frequency range like ^{13}C. (The length of the 90° pulse in paper I was 9.68 μs.) (iii) For absolute quantification purposes the signals should be acquired under non-saturation conditions. This means that the repetition time between the pulses should be five times the longest T_1 of the peaks to be measured. It is also possible to run under steady state conditions (repetition time < 5 x T_1), and then do T_1 corrections afterwards. The T_1 values for protons in water-soluble metabolites are normally between one and two seconds. However, it was of interest to measure if this was the case for the metabolites analysed in paper I.

Experimental description

Lens extract from one adult New Zealand albino rabbit were used. The PCA extraction was performed as described in paper I. The NMR spectra were obtained with a Bruker AVANCE DRX500 spectrometer operating at 500 MHz for protons. The ^{1}H spectra were recorded at 25°C using a 5 mm NMR tube, no spinning. Proton spectra were acquired using a 90° pulse and a spectral width of 5000 Hz. A standard inversion recovery sequence was used ($180_x° - \tau - 90_x°$ - FID) with acquisition time of 2.28 s and repetition delay of 10 s. Each spectrum corresponded to the sum of 96 FIDs. The time interval (τ) between the 180 and 90 degree pulses increased from 10 ms to 10 s, and 24 data points were acquired for T_1 computation. The T_1 results are shown in Table 3.1.

Table 3.1 Longitudinal relaxation times (T_1) of a representative selection of metabolites extracted from rabbit lens, freeze dried and re-dissolved in D_2O. The relaxation time for TSP was determined separately in D_2O.

ppm	Metabolite	T_1 value (sec)
0	TSP	3.4
1.02	valine	1.0
1.33	lactate	2.1
1.46	alanine	1.7
1.92	acetate	1.2
2.35	glutamate	1.5
2.41	succinate	2.0
2.67	hypo-taurine	1.3
3.30	scyllo-insitol	2.2
4.06	myo-inositol	1.8

The T_1 values for the metabolites in the lens extracts seemed to vary between 1.0 to 2.2 s. Based on the total repetition delay of 9 s in paper I, most of the observed metabolites were allowed a proper relaxation between the pulses. However, the internal standard showed surprisingly high T_1 value of 3.4 s. and was partially saturated. The T_1 relaxation process is described by the derived Bloch equation (3-1):

$$M_z(t) = M_0(1 - e^{-\frac{t}{T_1}}) \qquad (3\text{-}1)$$

were M_z is the steady state magnetization, M_0 is the equilibrium magnetization, t is the repetition delay (τ) and T_1 the relaxation time. From the equation TSP has only been allowed a total relaxation of 93%. This correction factor was not used when calculating the metabolite concentrations published in paper I.

3.4 HR-MAS spectroscopy of intact lenses

The CPMG pulse sequence

Baseline distortions caused by the immobile protons of macromolecules like lipids or proteins can be attenuated by spin-echo methods to reveal low molecular weight metabolites. This is based on much faster spin-spin relaxation (small T_2 values) for the immobile protons compared with the mobile protons (high T_2 values). A normal

Hahn spin-echo sequence [$90_x°$- τ -$180_y°$- τ - FID] gives rise to spin-spin coupling related phase modulation of the resonances which complicates the spectrum and its quantification. The Carr-Purcell-Meiboom-Gill (CPMG) sequence [$90_x°$ - (τ -$180_y°$-τ)$_n$ - FID] however, eliminates spin-diffusion, corrects for offset effects of imperfect 90° angles and minimises phase modulation [97]. The value of τ should be << 1/J to prevent spin diffusion to occur. Total spin-echo time in the range 100 - 150 ms is usually sufficient to attenuate the broad resonances. For the 1D HR-MAS spectra present in paper II - IV a CPMG sequence was used where the delay τ was set to 1 ms and n = 72 loops, giving an effective echo time of 144 ms. In addition a selective presaturation pulse was applied to enhance the water suppression. Fig. 3.3 illustrates the effect of the CPMG sequence on the broad baseline resonances.

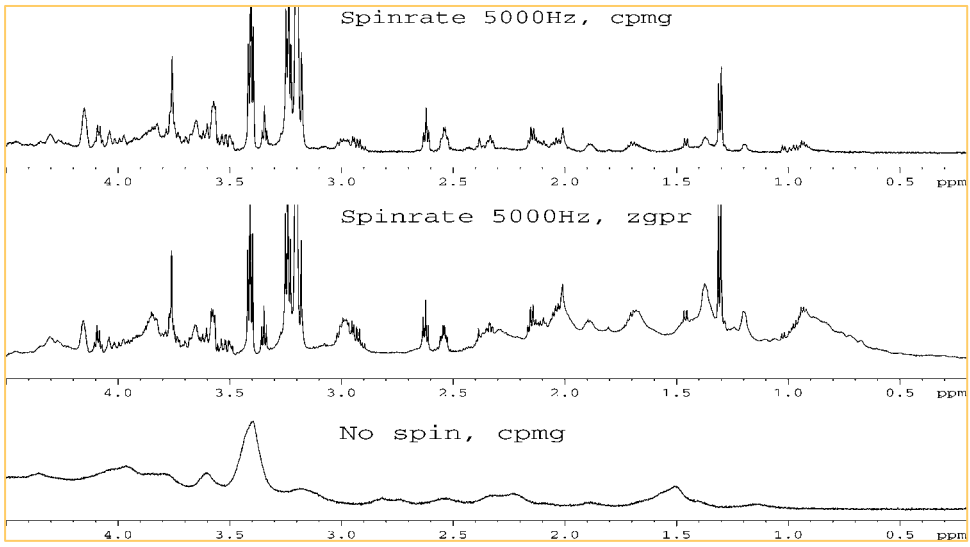

Figure 3.3 Representative MAS ^{1}H NMR spectra of intact rat lens tissue illustrating the effect of the rotor spin rate and the use of the T_2 filtering pulse technique (CPMG) with an effective echo time of 144 ms.

TSP as an internal standard

For the quantification of metabolites investigated by HR-MAS in paper II-IV it was difficult to use conventional methods with TSP as an internal standard. Firstly, the volume of standard solution added to each lens in the MAS rotor varied because of variations in the individual lens volume. When sealing the rotor containing the lens it was important to avoid air bobbles due to paramagnetic line broadening effects. Some liquid leakage in this process was unavoidable and total control of added TSP was

therefore difficult. Secondly, TSP possesses an aliphatic chain that can interact with serum albumin or lipids [98] and therefore might be unsuitable as internal standard for some biofluids (e.g. blood) and intact tissues. This did not seem to be a problem for the PCA tissue extracts and AH samples investigated in paper I, where TSP was used as internal standard.

Other internal standards like formate [98] and fumarate were considered. However, it was difficult to find a suitable reference that did not overlap with the endogenous metabolites in the lens, and the problem of adding the substrate to the rotor will still remain.

Another aspect regarding the use of TSP as a concentration standard is the relative long relaxation time (T_1 = 3.4s). This may be unfavourable when it is important to obtain sufficient S/N in low concentrated samples, with quantitative measurements within a reasonable amount of time [99].

T_2 measurements of metabolites from intact lens tissues

To investigate the relative differences in metabolite concentration between exposed and non-exposed lenses, measuring peak intensities versus noise ratios was found to be a suitable method (paper II and III). The same principle was used in paper IV only absolute peak intensities were used directly for comparison. The quantification methods utilised in paper II-IV was possible because all spectra were acquired and processed under identical conditions.

Quantification of the metabolites was based on the T_2 filtered spectra (CPMG). When interpreting the CPMG spectra for relative changes it was important that the metabolites had the same T_2 in normal and cataractous lenses. Cheng *et al.* [100] have shown that in some brain diseases consistency of metabolite T_2 relaxation cannot be assumed. If this is the case, some metabolites might be underrepresented due to short T_2. The T_2 values were examined for the 125 hrs post-irradiated lenses in paper III, and assumed to be representative for all the cataract experiments investigated in paper II-IV (Table 3.2).

Experimental description

Lenses from three six-week-old Brown Norway rats were used in this study. The lenses were prepared as described in paper III. One eye was exposed to 15 kJ/m^2 UVB radiation the contra lateral served as control. The rats were sacrificed 125 hrs post

exposure and lenses were removed. T_2 relaxation times of selected metabolites in the intact lenses were measured by HR-MAS ^{1}H NMR spectroscopy on a BRUKER Avance DRX600 spectrometer (14.1 Tesla, Bruker BioSpin GmbH) operating at 600 MHz for protons. The spectra were recorded at 4°C using a 4 mm HR-MAS ^{1}H/^{13}C probe. The spinning rate was 5 kHz. The spectra were acquired using a CPMG sequence as described above. The interpulse delay (τ) was 944.5 μs (rotor synchronized 180° pulses). Each spectrum corresponded to the sum of 96 FIDs. For the T_2 determination 32 data points were used which were acquired with 2τn varying from 32 – 1973 ms. Acquisition time was 2.5 s and the repetition delay 5.5 s. The relaxation evolution were analysed using the OriginLab 6.1 (MicroCal software, Northampton, U.S) program on a PC. The line fit model of the CPMG amplitudes was based on the equation (3-2), derived from Bloch equation, assuming a mono-exponential decay.

$$M_z(t) = M_0 \cdot e^{-\frac{t}{T_2}} \qquad (3\text{-}2)$$

Table 3.2 Transversal relaxation times (T_2) for different metabolites in intact rat lens present in milliseconds (ms).

		T_2 exposed (n = 3)	**T_2 control (n = 3)**
ppm	**Metabolite**	**ms ± SD**	**ms ± SD**
4.18	p-choline	538 ± 63	476 ± 18
4.06	m-inositol	248 ± 58	247 ± 22
3.42	taurine	585 ± 66	540 ± 98
2.57	GSH	321 ± 27	326 ± 6
2.41	succinate	242 ± 17	217 ± 7
2.35	glutamate	400 ± 27	395 ± 12
1.47	alanine	405 ± 66	351 ± 37
1.33	lactate	421 ± 15	424 ± 55
1.04	valine	342 ± 59	311 ± 64

The characteristic T_2 values are summarised in Table 3.2. The transversal relaxation processes for the metabolites were well described by a mono-exponential decay ($r^2 > 0.96$) and similar reports on brain metabolites also revealed mono-exponential properties [84], [53]. Attempts to describe a bi-exponential decay of the amplitudes

did not produce a significant better linefit. Further studies with a higher density of data points are needed to detect possible bi- or triple-exponential properties.

No significant differences in the T_2 values were observed between normal and cataractous lenses and it was assumed that this was the case for all the analysed changes present in paper II-IV. It should be mentioned that absolute quantification based on CPMG spectra require T_2 correction of the peak intensities based on accurate T_2 measurement of the respective metabolites.

3.5 Identification of the metabolites in NMR spectroscopy

The complex mixture of metabolites in biofluids and tissue requires careful analysis for identification of the individual metabolite contributions to the NMR spectra. Detailed information on different components is often hidden under unresolved multiplet groups exhibiting complex lineshapes and considerable spectral overlap.

In order to exhibit proper assignments of complex ^{1}H NMR spectra application of 2D NMR experiments are required.

The development of multidimensional NMR methods and stronger magnetic fields has greatly improved the potential of extracting information from complex mixtures such as crude tissue extracts. The most common 2D experiments for assignments of low-concentration metabolites are proton homonuclear correlated spectroscopy (H,H-COSY) and 2D J-resolved (JRES) (dispersion of the chemical shift and coupling constant data in two orthogonal frequency domains) experiments. However, overlapping resonances may still occur and additional 2D H,C-correlated experiments can be helpful to overcome these problems. Even though the sensitivity for heteronuclear correlation methods has been dramatically increased by the introduction of inverse-detected experiments like HSQC, HMQC and HMBC, it has been only scarcely used in metabolic studies of biological samples. In some pioneering reports heteronuclear 2D NMR have played a crucial role in providing considerable information on the chemical shifts of observable biomolecule resonances [54, 89, 90, 101, 102].

In interpretation of spectra from biofluids and tissues with limited S/N ratio it is however possible, to address most of the metabolite contributions by comparing traditional homonuclear 2D experiments with earlier reported shift resonances. In some cases it may be necessary to do additional spiking of the samples. The non-

destructive nature of NMR has also made it possible to confirm some assigned metabolites with chromatography methods after the NMR spectroscopy [93, 103].
Examples of earlier NMR studies on biological systems are: brain metabolites [103, 104], lipid and metabolite analysis of lymphocytes [93, 105], membrane lipids with special solvent systems [106], breast cancer tissue [55], intact human cell line [107], AH [76], cornea and lens extracts [77, 78] and testicular tissue [85].

All the ^{1}H NMR assignment work present in this thesis is based on literature search together with 2D COSY and JRES techniques. Attempts with 2D hetronuclear experiments like HSQC did not reveal any additional information due to low S/N ratio. Representative 2D spectra from HR-MAS experiments on rat lenses are given in Fig. 3.4-6. By comparing these data with reported assignments performed under the same physiologically relevant conditions (pH, temperature, solvent), detailed information on the contributing peaks in ^{1}H NMR spectra was obtained. Some metabolites also needed additional spiking to confirm their identity. The established chemical shift values for HR-MAS experiments on rat lenses, with reference to relevant shift values in literature, are given in Table 3.3.

Table 3.3 Chemical shift assignments from the HR-MAS ^{1}H NMR spectra of rat lens. Singlet, s; doublet, d; triplet, t; quartet, q; double doublet, dd; multiplet, m; not detected, ND; glycerophosphocholine, GPC; glycerophosphoethanolamine, GPE; reduced gluthatione, GSH; phospho-choline, p-choline. (a) Williker *et al*. [90] (b) Garrod *et al*. [54] (c) Nicholson *et al.* [101] (d) Podaniy *et al*. [108]

Label	Metabolite		Literature (δ ^{1}H)	This work	Label	Metabolite		Literature (δ ^{1}H)	This work
1	Acetate	β-CH_3	1.91 (s) [a]	1.92	14	Lysine	γ-CH_2	1.47 (m) [b]	1.49
							δ-CH_2	1.70 (m) [b]	1.69
2	Alanine	β-CH_3	1.46 (d) [c]	1.47			β-CH_2	1.90 (m) [b]	1.92
		α-CH	3.76 (q) [c]	3.79			ε-CH	3.02 (t) [b]	3.03
							α-CH	3.75 (t) [b]	3.76
3	Betaine	CH_3	3.26 (s) [b]	ND					
		CH_2	3.89 (s) [b]	3.92	15	Myo-inositol	C5H	3.28 (t) [b]	3.27
							C1, 3H	3.53 (dd) [b]	3.53
4	Citrate		2.52 (dd) [a]	2.55			C4, 6H	3.62 (t) [b]	3.62
			2.69 (dd) [a]	2.71			C2H	4.06 (t) [b]	4.08
5	Glutamine	β-CH_2	2.15 (m) [a]	2.13	16	Phe-alanine	β-CH	3.13 (dd) [b]	3.13
		γ-CH_2	2.46 (m) [a]	2.46			β'-CH	3.26 (dd) [b]	3.26
		α-CH_2	3.71 (t) [a]	3.79			α-CH	3.98 (dd) [b]	4.00
							C3,5H ring	7.32 (m) [b]	7.32
6	Glutamate	β-CH_2	2.06 (m) [a]	2.08			C2,6H ring	7.40 (m) [b]	7.41
		γ-CH_2	2.34 (m) [a]	2.35					
		α-CH_2	3.77 (t) [a]	3.78	17	P-choline	N-CH_2	3.59 (m) [a]	3.60
							O-CH_2	4.15 (m) [a]	4.18
7	Glycine	α-CH	3.54 (s) [c]	3.55			$N(CH_3)_3$	3.21 (s) [e]	3.22
8	GPC	N-CH_2	3.67 (?) [a]	3.69	18	Succinate		2.39 (s) [a]	2.41
		O-CH_2	4.32 (?) [a]	4.34					
					19	Taurine	N-CH_2	3.25 (t) [a]	3.25
9	GPE	N-CH_2	3.29 (?) [a]	3.18			S-CH_2	3.41 (t) [a]	3.42
		O-CH_2	4.11 (?) [a]	4.12					
					20	Threonine	γ-CH_3	1.32 (d) [b]	1.33
10	GSH	Glu 2	3.77 (t) [d]	3.79			β-CH	4.26 (m) [b]	4.26
		Glu 3	2.15 (m) [d]	2.16			α-CH	3.58 (d) [b]	3.58
		Glu 4	2.53 (m) [d]	2.57					
		Glu 4	2.55 (m) [d]	2.57	21	Tyrosine	β-CH	3.02 (dd) [a]	3.05
		Gly 2	3.79 (s) [d]	ND			β'-CH	3.20 (dd) [a]	3.21
		Cys 2	4.56 (dd) [d]	4.59			α-CH	3.89 (dd) [a]	3.98
		Cys 3	2.92 (dd) [d]	2.94			C3,5H ring	6.89 (d) [a]	6.89
		Cys 3	2.95 (dd) [d]	2.95			C2,6H ring	7.19 (d) [a]	7.18
11	Hypo-taurine	N-CH_2	2.64 (t) [a]	2.65	22	Valine	γ-CH_3	0.97 (d) [b]	0.98
		S-CH_2	3.36 (t) [a]	3.36			γ-CH_3	1.02 (d) [b]	1.04
							β-CH	2.28 (m) [b]	2.27
12	Lactate	β-CH_3	1.32 (d) [c]	1.33			α-CH	3.61 (d) [b]	3.62
		α-CH	4.11 (q) [c]	4.12					
13	Leucine	δ'-CH_3	0.94 (d) [b]	0.95					
		δ-CH_3	0.96 (d) [b]	0.97					
		β-CH_3	1.70 (m) [b]	1.71					
		γ-CH_2	1.66 (m) [b]	1.65					
		α-CH	3.70 (t) [b]	ND					

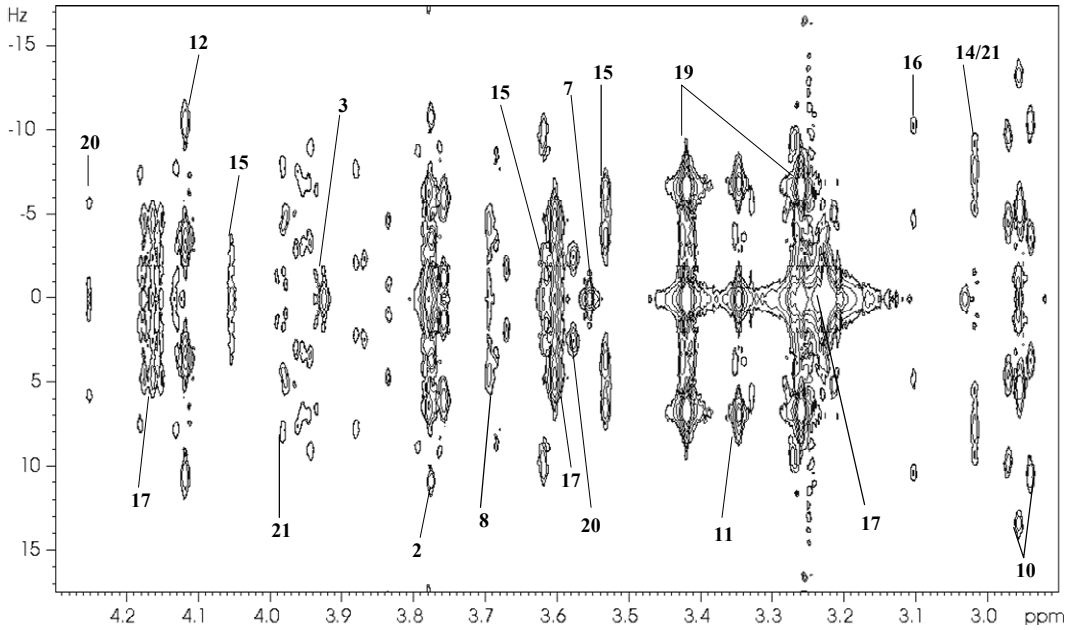

Figure 3.4 A representative JRES MAS ^{1}H NMR spectrum of a normal rat lens (δ 2.9 – 4.3 ppm). Spin rate 5000 Hz. The assignment numbers are given in Table 3.3.

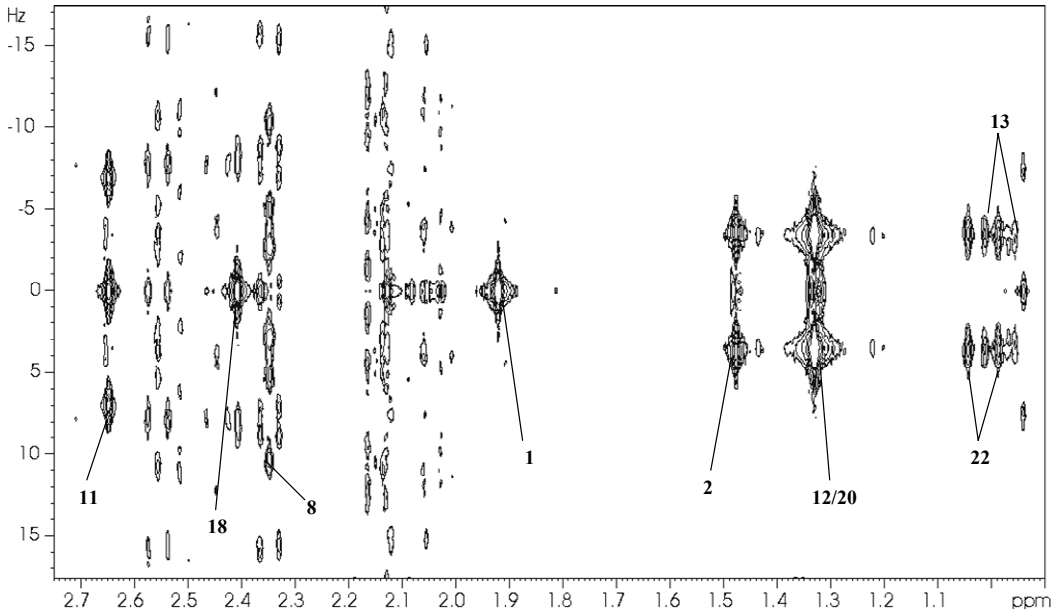

Figure 3.5 A representative JRES MAS ^{1}H NMR spectrum of a normal rat lens (δ 0.8 – 2.75 ppm). Spin rate 5000 Hz. The assignment numbers are given in Table 3.3.

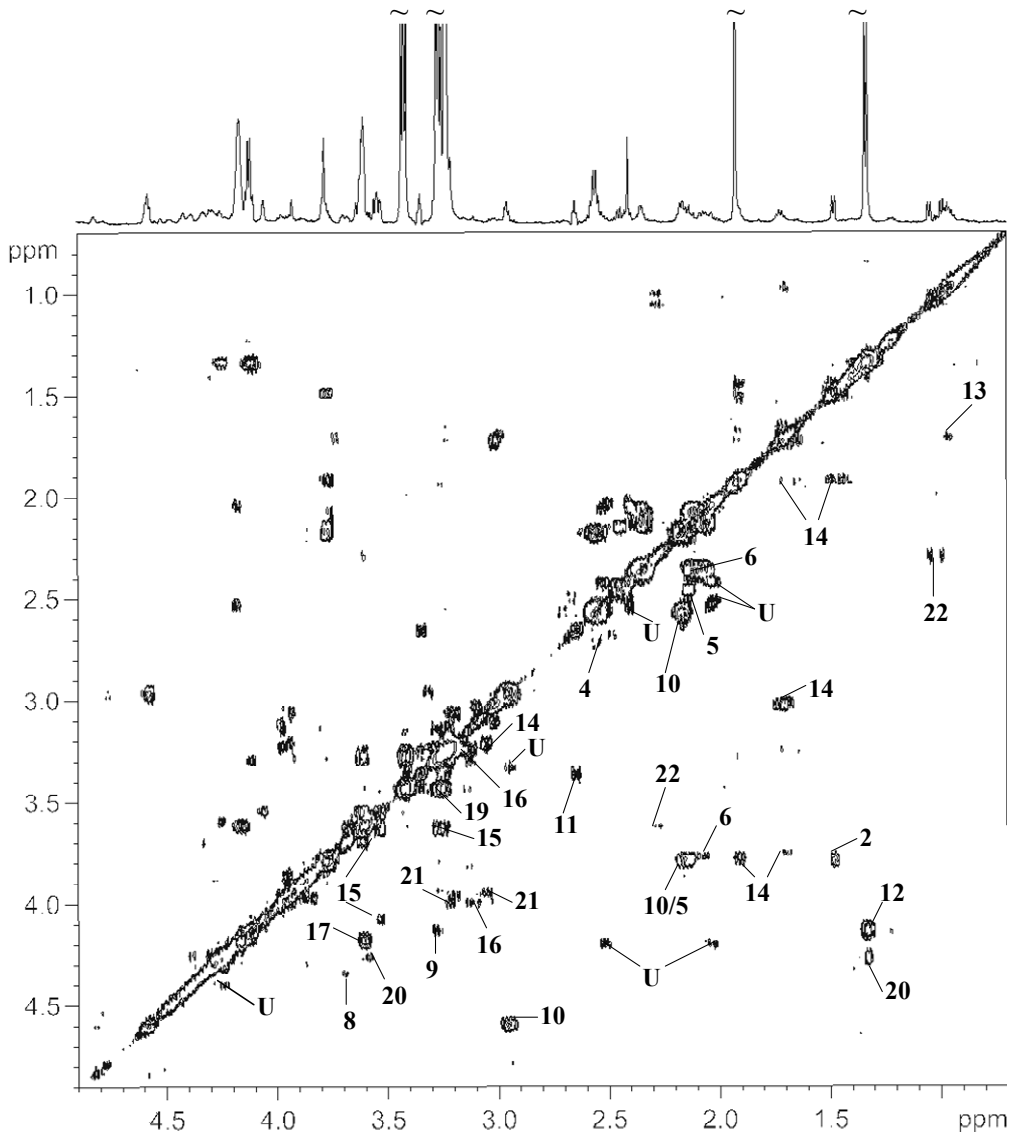

Figure 3.6 Partial (δ 4.9 - 0.7 ppm) ^{1}H- ^{1}H COSY MAS NMR spectrum of a normal rat lens with the skyline one-dimensional projection of a CPMG spectrum. Spin rate 5000 Hz. Unknown, (U). The assignment numbers are given in Table 3.3.

4. Results and Discussion

4.1 Paper I

Analysis of immediate changes of water-soluble metabolites in alkali-burned rabbit cornea, aqueous humor and lens by high-resolution ^{1}H NMR spectroscopy

The aim of this study was to use high-resolution ^{1}H NMR spectroscopy to access information of the immediate metabolic changes in the anterior eye segment after alkali-burn. Previous studies of alkali-burn injuries have focused on wound healing and enzyme activity, investigated mainly on the long-term changes. Less attention has been paid to the immediate metabolite changes that occur. These changes might be crucial for the later development of biochemical healing processes.

By using high-resolution ^{1}H NMR spectroscopy on the eye tissue PCA extracts, it was possible to simultaneously detect and quantify many different metabolites without demanding chemical derivatisation methods. In addition to 2D NMR experiments and earlier reported NMR assignments of complex biological extracts [89, 101, 109], previous ^{1}H NMR spectroscopy work from our laboratory on metabolic analysis of cornea [77], aqueous humour [76] and lens [78] was used as a platform for peak assignments of the obtained ^{1}H NMR spectra.

A total of 22 different metabolites were quantified in cornea, AH and lens (Fig. 2-5, paper I), varying in concentration from 0.02 to 23.47 mmol/kg wet weight. Observed concentrations of lactate and glucose in cornea corresponded well with previous findings [110]. The most prominent metabolite in all three eye tissues was lactate, which showed an overall increase after alkali-burn. This might indicate an ischemic process [21]. Significant change in lactate concentration was observed as far in as the lens, indicating that alkali-burn causes rapid metabolic alteration deep into the anterior segment of the eye. Hypo-taurine, a precursor of taurine, decreased significantly in cornea. Taurine's functions, both as osmolyte and antioxidant, [111] might be affected by the decrease of hypo-taurine. The most significant changes in concentrations were found in AH with significant increase in succinate, creatine, scyllo-inositol and myo-inositol, and a significant decrease of citrate. Also ascorbate showed a non-significant decrease in AH. Previous studies have demonstrated the

benefit of ascorbate and citrate in the treatment of alkali-burns in the eye, reducing the amount of corneal damage [16, 17, 112]. The increase in inositol concentrations may reflect a destruction of cell membranes [113]. However it has been shown that inositol may also function as an osmoregulator [114, 115]. This paper showed that ^{1}H NMR spectroscopy was well suited to provide both quantitative and qualitative information on changes in metabolite concentrations in damaged tissues. Thus ^{1}H NMR spectroscopy might be helpful to evaluate and understand the biological alterations due to external noxi like alkali-burns.

4.2 Paper II

Metabolic changes in rat lens after *in vivo* exposure to ultraviolet irradiation: measurements by high-resolution MAS ^{1}H NMR spectroscopy

The aim of this study was to implement HR-MAS ^{1}H NMR spectroscopy as an analytical tool for use on intact lenses, and apply the technique to investigate changes in the metabolic profile of intact rat lenses after *in vivo* UVB radiation. Despite the many experimental studies of UVR and cataract development, the metabolic changes involved in this process are not clear. In this study it was of interest to investigate if endogenous metabolite alterations followed dose response relationship similar to that reported for lens opacity and UVB exposure.

Previous experiments in our laboratory have found ^{1}H NMR spectroscopy to be very useful in the monitoring of metabolic profiles in tissue extracts (paper I). However, analysis of extracts requires relatively large amounts of biological tissue, are time consuming, and may change the chemical composition of the sample. The present paper introduced for the first time high-resolution ^{1}H NMR spectroscopy on intact lens tissue. The obtained HR-MAS ^{1}H NMR spectra were of high quality comparable to those from lens tissue extracts in paper I. Carefully assignment analysis based on 2D NMR experiments and previous assignment studies of extracts [78, 90, 101, 104] and intact tissue [54] were done, and it was possible to identify more than 30 different metabolites in the spectra. Sixteen metabolites qualified to quantitative measurements; taurine, hypo-taurine, tyrosine, phenylalanine, valine, glycine,

glutamate, alanine, myo-inositol, p-choline, betaine, succinate, GSH, ATP&ADP, AMP and lactate (Fig. 3, paper II).

The mean forward light scattering increased with increasing UVR dose. It was shown that near-threshold UVB doses lead to a general significant decrease in water-soluble metabolites, one week after exposure. However no dose-dependent changes in the metabolites were observed.

The general decrease in metabolite concentrations in the lens might indicate a leakage of water-soluble metabolites due to membrane damage caused by UVB radiation. Hightower *et al.* [116] have shown that UVR induces changes in membrane permeability which further lead to osmotic stress. In the lens particularly taurine and myo-inositol are involved in the osmotic regulation [114, 115], and in the present paper taurine, hypo-taurine and myo-inositol are among the metabolites with the largest decrease in concentration.

GSH, which is involved in protection of oxidative damage and cell membrane transport, showed a significant decrease between 20 and 50%. This was supported by earlier studies on lens epithelial cells, showing that the GSH level stabilised 15 to 20% below normal level when exposed to oxidative stress [117].

A significant reduction in ATP and ADP combined with an increase in AMP indicated that lenticular damage or stress result in increased energy demands. Similar responses in energy metabolism have been reported for other experimental stressors such as calcium deprivation [118], steroid treatment [66, 119] and galactose-induced cataract [120].

This study demonstrated the potential of HR-MAS ^{1}H NMR spectroscopy as an analytical tool for use on intact lenses. The fact that some metabolites decreased more than others implicates their different roles in protection of the lens against UVB radiation, and illustrates the complexity of this process and the effect on the metabolic changes.

4.3 Paper III

Time dependency of metabolic changes in rat lens after *in vivo* UVB irradiation analysed by HR-MAS ^{1}H NMR spectroscopy

In paper II it was suggested that the lack of dose-dependent changes in the metabolites might be explained by repair processes during the first week after UVB radiation.
The aim of this study was to investigate the time-dependent metabolic changes 5 to 625 hrs after UVB radiation. Knowledge of the metabolic profile in the lens at different stages in the cataract development may contribute to a better understanding of how the metabolism is influenced by UVB exposure.

As shown in paper II the non-destructive technique, HR-MAS spectroscopy, made it possible to obtain high-resolution ^{1}H NMR spectra of intact rat tissue. In this study pigmented rats were exposed to threshold UVB doses comparable to the experiments on albino rats in paper II. The observed increase in light scattering in the lens after UVB radiation was transient, showing a maximum at 25 hrs post exposure. However, the major changes observed in the metabolic profile peaked after a 125 hrs latency time, showing that the irradiation impact on the metabolic profile did not follow the same time-dependency as the development of light scattering. The only significant change observed at an earlier stage was a decrease in ATP/ADP 5 hrs after UVB radiation. The peak changes in the endogenous metabolite concentrations at 125 hrs post exposure support previous observations that the lens is more vulnerable to additional UVB attacks a certain time after exposure [121]. The delayed time response of the concentration changes indicate that initial changes in the lens epithelium [45, 122] might induce additional biochemical changes to the bulk of the lens at a later stage. Both light scattering and the metabolite concentrations seemed to converge back to normal after 625 hrs.
Like in paper II a general decrease in the water-soluble metabolite concentrations was observed after UVB radiation. Significant decrease in osmolytes like taurine and myo-inositol indicated a loss of homeostasis and osmotic stress [116]. Michael *et al.* [44] observed that UVB radiation induced apoptosis in the lens epithelial cells, and other studies have reported a relationship between apoptosis and extrusion of organic osmolytes [123]. Previous studies have also shown that osmotic and oxidative stress caused an increased efflux of lenticular organic phosphate compounds [124, 125]

including p-choline that revealed a significant decrease 125 and 625 hrs after UVB radiation in present study.
Also the level of betaine, known as a dominating osmolyte in placenta and renal medulla [126], fell significantly 125 hrs post exposure. So far, no osmolytic activity has been reported for betaine in the lens [126], but betaine may have other roles such as stabilising effects on macromolecules [127]. Our laboratory is the first to report a biological response of betaine concentration in the lens.
Phenylalanine was the only metabolite that showed a significant increase. Valine and alanine showed a non-significant increase 125 hrs post exposure.

Like in paper II the diverse response of the metabolites implicated their different role in the lenticular damage and repair processes after threshold doses of UVB radiation. This study emphasized the strength of HR-MAS spectroscopy in screening multiparametric responses in intact lens tissue to drugs or pathophysiological stimuli.

4.4 Paper IV

High-resolution magic angle spinning ^{1}H NMR spectroscopy of metabolic changes in rabbit lens after treatment with dexamethasone combined with UVB exposure

The purpose of this study was to investigate metabolic changes in the rabbit lens after combined treatment with dexamethasone and UVB exposure, using HR-MAS ^{1}H NMR spectroscopy to analyse intact lens tissues. Cataract formation is a well established side effect of long-term treatment with steroids. However, cataract formation is a multifactorial process and it was of interest to investigate if short-term UVB radiation had additive effects on the metabolic changes in the lens.

The spectra were acquired from a section of each rabbit lens containing both cortical and nuclear parts, giving an average metabolic profile of each lens. Signals from more than 15 major metabolites were assigned (Fig. 1, paper IV), including glucose, sorbitol, sorbitol-3-phosphate and scyllo-inositol that were not detectable in rat lenses in paper II and III. However, glucose was only detected in the rabbit lenses after long-term treatment with dexamethasone combined with a subsequent UVB exposure.

High levels of glucose in the lens may lead to activation of aldose reductase [128, 129] and concomitantly polyol accumulation [130].
In addition a significant concentration decrease in GSH, myo-inositol, scyllo-inositol, choline, lactate and valine, and an increase in alanine were detected after the combined treatment. Further 2D spectral interpretation (Fig. 2, paper IV) also revealed a large decrease in taurine and an increase in sorbitol and sorbitol-3-phosphate. However, this was not exactly quantifiable due to severe spectral overlap. In experimental diabetic conditions taurine depletion has been observed in response to the accumulation of sorbitol within the lens [131]. It has also been shown that polyol accumulation induced myo-inositol release from the lens epithelial cells [132]. Thus, the observed depletion in taurine and inositols in the present paper might indicate an osmotic compensation in response to the accumulation of sorbitol.
Regarding the observed decrease of the vital lens antioxidant GSH [133] in the combined treatment, it has previously been suggested that glucocorticoid activity is responsible for loss in lenticular GSH [134] thereby leading to cataractogenesis [135].

For UVB irradiation alone, only glutamate and lactate showed significant changes. The metabolic state of the lens was affected more profoundly by long-term steroid treatment than by short-term UVB exposure. However, Pescosolido *et al*. [82] did not find any change in lenticular lactate concentration after long-term dexamethasone treatment of rabbit eyes. This might indicate that the decreased lactate concentration in present study was caused by the UVB radiation. Reduced lactate level might be due to inactivation of glycolytic enzymes after UVB exposure [41, 42].
This study showed that high quality spectra can be obtained from small lenticular sections. By implementing improved sectioning techniques, HR-MAS spectroscopy should enable future work to investigate the metabolites from different parts of the lens.

5. Concluding remarks

The ^{1}H NMR spectra of both eye tissue extracts and intact lenses in this thesis show an extensive picture of NMR detectable metabolites. In addition to the detailed analysis of AH and tissue extracts from cornea and lens, this work has created a basis for implementation and interpretation of HR-MAS ^{1}H NMR spectroscopy on intact lens tissues, and provided a future platform for the investigation of intact eye tissues in general. The analysis of endogenous metabolites of intact tissues from the anterior eye segment might enable new bridges to be constructed between ophthalmic biochemistry research and conventional histopathology. The metabolic profiles obtained *in vitro* may also be important for future applications and interpretation of ^{1}H NMR spectroscopy *in vivo*.

Differences in the metabolic content in cornea, AH, and lens after alkali-burns to the eye were established in paper I. This showed how careful ^{1}H NMR spectroscopy analysis of tissue extracts provided new information (quantitative and qualitative) on the metabolic reaction pattern in the anterior eye segment in relation to eye alkali burn injuries. The peak assignments of the NMR spectra obtained in these extract experiments were also important for the subsequent investigation of intact lens tissues in paper II-IV.

In the HR-MAS studies in paper II-IV particular attention was paid to metabolic alterations occurring by the development of lens opacities and cataracts. The T_2 values of water-soluble metabolites in the lens did not change significantly in opaque lenses, making the T_2 filtering CPMG pulse technique reliable in relative quantitative analysis of normal and cataractous lenses.

In paper II the close-to-threshold UVB doses did not reveal any dose-response relationship for the metabolic changes. However, the significant decrease in concentration for most of the observed metabolites seven days post exposure demonstrated that moderate UVB radiation had great impact on the metabolites in the lens.

Studies of time dependent impact of UVB radiation in paper III showed that changes in metabolite concentrations were delayed compared to the development of lens opacities. Most of the significant changes seemed to converge back to normal values 625 hrs (26 days) after exposure.

No clear cataract was detected after long-term steroid treatment combined with UVB exposure in paper IV. However, significant changes were observed for several metabolites. Long-term steroid treatment seemed to have greater impact on the metabolic changes in the lens than short-term changes induced by UVB radiation. For some metabolites the induced changes seemed to be additive. Paper IV also illustrated how 2D experiments aid the extraction of information in crowded regions of the spectra with high degree of overlap.

6. Future perspectives

A detailed ^{1}H NMR assignment study of metabolites in the lipid fraction from M/C extracts of the lens should be performed. Unpublished 1D ^{1}H NMR spectra of the lipid fraction from our lab revealed several unassigned peaks, but also broad resonances from macromolecules that need to be suppressed.

The application of multivariate statistical methods may be helpful to extract additional biological data in complex parts of the spectra that is not revealed by visual inspection. Data reduction of NMR spectra and pattern recognition techniques are widely used in metabolite studies, an approach comprised by metabonomics [51, 136, 137].
Analysis based on multivariate methods of NMR spectra from intact eye tissue should be done to see if it is possible to extract further information on metabolite changes.

The studies in paper II should be extended to higher and lower UVB doses with concomitant time-dependent studies of the metabolic profile, to investigate if threshold doses for the metabolic changes in the lens might exist.

The metabolic analysis in present thesis was confined to the whole lens (paper I-III), or a part representative for the whole lens (paper IV), and has not been directed towards possible local variations in the lens. It is believed that most of the UVB radiation is absorbed in the anterior part of the lens. Thus metabolites present in the anterior part are more exposed to UVB radiation than metabolites in the posterior part. In addition proteins [138, 139] and enzymes [140, 141] are not homogenously distributed within the lens. In special cases it is possible that analysis of the whole lens would fail to detect significant changes. Thus in the future, biochemical comparisons made by HR-MAS ^{1}H NMR spectroscopy should be done on different sections of the lens. The spectra of small lenticular sections from rabbit lenses in paper IV showed that this should be possible.

The application of ^{1}H NMR spectroscopy on intact eye tissues also opens for analysis of other physical properties like compartmentation or diffusion of water and small metabolites. The relaxation parameters T_1 and T_2 provide information on the

interaction between water/metabolites and macromolecules like proteins and lipids. Several relaxation and diffusion studies have been performed both on normal and cataractous lenses [142-147]. However HR-MAS spectroscopy opens new possibilities to similar investigation of small metabolites within the lens [56]. Combined with regional analysis it should be possible to monitor mobility of the metabolites within their respective localisations and how they may be affected by different pathological conditions.

One of the future aims should also be to perform absolute quantification of the metabolites in intact tissue by using HR-MAS NMR spectroscopy.

It would be interesting to do comparative metabolite analysis of albino versus pigmented, and young versus old rats, and further compare the metabolic profile of eye tissues in animal models to human tissues.

7. References

1. Forrester J.V., Andrew D.D., McMenamin P.G. and Lee W.R. (2002) The eye; basic science in practice. Edited by Parkinson M. W. B. Saunders, London.
2. Maurice D.M. (1984) The Cornea and Sclera. The Eye. Edited by Davson H. Academic Press, New York. pp 1-158.
3. Huang K. and Meek K.M. (1999) Swelling studies on the cornea and sclera: the effects of pH and ionic strength. *Biophys J* 77, 1655-1665.
4. Shioda R., Reinach P.S., Hisatsune T. and Miyamoto Y. (2002) Osmosensitive taurine transporter expression and activity in human corneal epithelial cells. *Invest Ophthalmol Vis Sci* 43, 2916-2922.
5. Fischern T.v., Lorenz U., Burchard W.G., Reim M. and Schrage N.F. (1998) Changes in mineral composition of rabbit corneas after alkali burn. *Graefe's Arch Clin Exp Ophthalmol* 236, 553-558.
6. Lu L., Reinach P.S. and Kao W.W.Y. (2001) Corneal epithelial wound healing. *Exp Biol Med* 226, 653-664.
7. Reim M., Busse S., Leber M. and Schulz C. (1988) Effect of epidermal growth factor in severe experimental alkali burns. *Ophthal Res* 20, 327-331.
8. Reim M. and Becker J. (1995) New strategies in prevention and therapy: Cell protection in the anterior segment of alkali-burnt eyes. Edited by Schmidt K. Hippokrates Verlag, Stuttgart. pp 49-54.
9. Kolozsvari L., Nogradi A., Hopp B. and Bor Z. (2002) UV absorbance of the human cornea in the 240- to 400-nm range. *Invest Ophthalmol Vis Sci* 43, 2165-2168.
10. Tsubia T. and Matsuo M. (2002) Ultraviolet light-induced changes in the glucose-6-phosphate dehydrogenase activity of porcine corneas. *Cornea* 21, 495-500.
11. To C.H., Kong C.W., Chan C.Y., Shahidullah M. and Do C.W. (2002) The mechanism of aqueous humour formation. *Clin Exp Optomet* 85, 335-349.
12. Brubaker R.F. (1991) Flow of aqueous-humor in humans - the Friedenwald lecture. *Invest Ophthalmol Vis Sci* 32, 3145-3166.
13. Ringvold A. (1996) The significance of ascorbate in the aqueous humour protection against UVA and UVB. *Exp Eye Res* 62, 261-264.
14. Ringvold A. (1980) Aqueous humour and ultraviolet radiation. *Acta Ophthalmol (Copenh)* 58, 69-82.
15. Tessem M.-B., Bathen T.F., Cejková J. and Midelfart A. (2004) Effect of UVA and UVB irradiation on the metabolic profile of aqueous humour in rabbits analysed by ^{1}H NMR spectroscopy. *Submitted to Invest Ophthalmol Vis Sci*
16. Levinson R.A., Paterson C.A. and Pfister R.R. (1976) Ascorbic acid prevents corneal ulceration and perforation following experimental alkali burns. *Invest Ophthalmol* 15, 986-993.

17. Pfister R.R. and Paterson C.A. (1980) Ascorbic acid in the treatment of alkali burns of the eye. *Ophthalmol* 87, 1050-1057.
18. Pfister R.R. (1983) Chemical injuries of the eye. *Ophthalmology* 90, 1246-1253.
19. Midelfart A., Hagen Y.C. and Myhre G.B.S. (2004) Etseskader på øyet. *Tidsskr Nor Lægeforen* 1, 49-51.
20. Nelson J.D. and Kopietz L.A. (1987) Chemical Injuries to the Eyes. *Ocular burns* 81, 62-75.
21. Reim M. (1992) The results of ischaemia in chemical injuries. *Eye* 6, 376-380.
22. Belin M.W., Catalano R.A. and Scott J.L. (1992) Burns of the eye. Ocular Emergenica. Edited by Catalano R.A. W.B. Saunder Co. pp 179-196.
23. Reim M., Bahrke C., Kuckelkorn R. and Kuwert T. (1993) Investigation of enzyme activities in severe burns of the anterior eye segment. *Graefe's Arch Clin Exp Ophthalmol* 231, 308-312.
24. Čejková J., Lojda Z., Salonen E.-M. and Vaheri A. (1989) Histochemical study of alkali-burned rabbit anterior eye segment in which severe lesions were prevented by aprotinin treatment. *Histochem* 92, 441-448.
25. McCarty C.A. and Taylor H.R. (1996) Recent developments in vision research: light damage in cataract. *Invest Ophthalmol Vis Sci* 37, 1720-1723.
26. Hockwin O., Kojima M., Müller-Breitenkamp U. and Wegner A. (2002) Lens and cataract research of the 20th century: a review of results, errors and misunderstandings. *Dev Ophthalmol* 35, 1-11.
27. Harding J.J. and Crabbe M.J.C. (1984) The lens: development, proteins, metabolism and cataract. The Eye. Edited by Davson H. Academic Press, Orlando. pp 207-492.
28. Brown K.S. (1999) The ozone layer: burnt by the sun down under. *Science* 285, 1647-1649.
29. Sasaki H., Kawakami Y., Ono M., Jonasson F., Shui Y.B., Cheng H.-M., Robman L., McCarty C., Chew S.J. and Sasaki K. (2003) Localization of cortical cataract in subjects of diverse races and latitude. *Invest Ophthalmol Vis Sci* 44, 4210-4214.
30. Taylor H.R., West S.K., Rosenthal F.S., Munoz B., Newland H.S., Abbey H. and Emmet E.A. (1988) Effect of ultraviolet radiation in cataract formation. *N Engl J Med* 319, 1429-1433.
31. McCarty C.A. and Taylor H.R. (2002) A review of the epidemiologic evidence linking ultraviolet radiation and cataracts. *Dev Ophthalmol* 35, 21-31.
32. Merriam J.C., Löfgren S., Michael R., Söderberg P., Dillon J., Zheng L. and Ayala M. (2000) An action spectrum for UVB radiation and the rat lens. *Invest Ophthalmol Vis Sci* 41, 2642-2647.
33. Pitts D.G., Cullen A.P. and Hacker P.D. (1977) Ocular effects of ultraviolet radiation from 295 to 365 nm. *Invest Ophthalmol Vis Sci* 16, 932-939.
34. Oriowo O.M., Cullen A.P., Chou R.B. and Sivak J.G. (2001) Action spectrum and recovery for in vitro UV-induced cataract using whole lenses. *Invest Ophthalmol Vis Sci* 42, 2596-2602.
35. Taylor A. and Davies K.J.A. (1987) Protein oxidation and loss of protease activity may lead to cataract formation in the aged lens. *Free Radic Biol Med* 3, 371-377.

36. Edwards A.M. and Silva E. (2001) Effect of visible light on selected enzymes, vitamins and amino acids. *J Photochem Photobiol B* 63, 126-131.

37. Reddy V.N. (1990) Glutathione and its function in the lens - An overview. *Exp Eye Res* 50, 771-778.

38. Kilic F., Bhardwaj R., Caulfield J. and Trevithick J.R. (1999) Modelling cortical caractogenesis 22: is in vitro reduction of damage in model diabetic rat cataract by taurine due to its antioxidant activity? *Exp Eye Res* 69, 291-300.

39. Reddy V.N., Giblin F.J., Lin L.-R. and Chakrapani B. (1998) The effect of aqueous humor ascorbate on ultraviolet-B-induced DNA damage in lens epithlium. *Invest Ophthalmol Vis Sci* 39, 344-350.

40. Truscott R.J.W., Wood A.M., Carver J.A., Sheil M.M., Stutchbury G.M., Zhu J. and Kilby W. (1994) A new UV-filter compuond in human lenses. *FEBS Lett* 348, 173-176.

41. Löfgren S. and Söderberg P.G. (2001) Lens lactate dehydrogenase inactivation after UVB irradiation: an in vivo measure of UVR-B penetration. *Invest Ophthalmol Vis Sci* 42, 1833-1836.

42. Löfgren S. and Soderberg P.G. (1995) Rat lens glycolysis after in vivo exposure to narrow band UV or blue light radiation. *J Photochem Photobiol B* 30, 145-151.

43. Hightower K.R., McCready J.P. and Brochman D. (1994) Membrane damage in UVB irradiated lenses. *Photochem Photobiol* 59, 485-490.

44. Michael R., Vrensen G.F.J.M., Marle J.v., Gan L. and Söderberg P.G. (1998) Apoptosis in the rat lens after in vivo threshold dose ultraviolet irradiation. *Invest Ophthalmol Vis Sci* 39, 2681-2687.

45. Li W.-C. and Spector A. (1996) Lens epithelial cell apoptosis is an early event in the development of UVB-induced cataract. *Free Radic Biol Med* 20, 301-311.

46. Michael R. (2000) Development and repair of cataract induced by ultraviolet radiation. *Ophthalmic Res* 32, 1-45.

47. Bloch F., Hansen W.W. and Packard M. (1946) Nuclear induction. *Phys Rev* 69, 680.

48. Purcell E.M., Torrey H.C. and Pound R.V. (1946) Resonance absorption by nuclear magnetic moments in a solid. *Phys Rev* 69, 37-38.

49. Friebolin H. (1998) Basic one- and two-dimensional NMR spectroscopy. Edited by Friebolin H. Wiley-VCH Verlag GmbH, Weinheim.

50. Claridge T.D.W. (1999) High-resolution NMR techniques in organic chemistry. Edited by Baldwin J.E. and Williams R.M. Pergamon Press Ltd, Oxford.

51. Lindon J.C., Holmes E. and Nicholson J.K. (2003) So what's the deal with metabonomics. *Anal Chem* 75, 384A-391A.

52. Moka D., Vorreuther R., Schicha H., Spraul M., Humpfer E., Lipinski M., Foxall P.J.D., Nicholson J.K. and Lindon J.C. (1997) Magic angle spinning proton nuclear magnetic resonance spectroscopic analysis of intact kidney tissue samples. *Analyt Communic* 34, 107-109.

53. Cheng L.L., Chang I.W., Smith B.L. and Gonzalez R.G. (1998) Evaluating human breast ductal carcionomas with high-resolution magic-angle spinning proton magnetic resonance spectroscopy. *J Magnet Reson* 135, 194-202.

54. Garrod S., Humpfer E., Spraul M., Connor S.C., Polley S., Connelly J., Lindon J.C., Nicholson J.K. and Holmes E. (1999) High-resolution magic angle spinning ^{1}H NMR spectroscopic studies on intact rat renal cortex and medulla. *Magn Reson Med* 41, 1108-1118.

55. Sitter B., Sonnewald U., Spraul M., Fjösne H.E. and Gribbestad I. (2002) High-resolution magic angle spinning MRS of breast cancer tissue. *NMR Biomed* 15, 327-337.

56. Rooney O.M., Troke J., Nicholson J.K. and Griffin J.L. (2003) High-Resolution diffusion and relaxation-edited magic angle spinning ^{1}H NMR spectrscopy of intact liver tissue. *Magn Reson Med* 50, 925-930.

57. Kopp S.I., Greiner J.V. and Glonek T. (1981) Analysis of intact rat lens metabolites by ^{31}P NMR spectroscopy. *Curr Eye Res* 1, 375-381.

58. Greiner J.V., Kopp S.J., Sanders D.R. and Glonek T. (1981) Organophosphates of the crystalline lens: a nuclear magnetic resonance spectroscopic study. *Invest Ophthalmol Vis Sci* 21, 700-713.

59. Greiner J.V., Kopp S.J., Gillette T.E. and Glonek T. (1983) Phosphatic metabolites of the intact cornea by ^{31}P nuclear magnetic resonance. *Invest Ophthalmol Vis Sci* 24, 535-542.

60. Greiner J.V., Chanes L.A. and Glonek T. (1991) Comparsion of phosphate metabolites of the ocular humors. *Ophthalmic Res* 23, 92-97.

61. Cheng H.M. (1989) Cornea-soft contact-lens interaction - a nuclear magnetic resonance study. *Optom Vis Sci* 66, 515-517.

62. Tsubota K., Kenyon K.R. and Cheng H.M. (1989) Hard contact lens-induced metabolic changes in rabbit corneas. *Exp Eye Res* 49, 769-775.

63. Hayashi K., Cheng H.M., Xiong J., Xiong H. and Kenyon K.R. (1989) Metabolic changes in the cornea of vitamin-A-deficient rats. *Invest Ophthalmol Vis Sci* 30, 769-772.

64. McCartney M.D., Thomas D.M. and Mahendroo P.P. (1992) An electron microscopic and nuclear magnetic resonance spectroscopic evaluation of rabbit corneal ephithelial wound healing. *Invest Ophthalmol Vis Sci* 33, 2917-2925.

65. Lerman S., Ashley D.L., Long R.C., Goldstein J.H., Megaw J.M. and Gardner K. (1982) Nuclear magnetic resonance analyses of the cold cataract: whole lens studies. *Invest Ophthalmol Vis Sci* 23, 218-226.

66. Greiner J.V., Kopp S.J. and Glonek T. (1982) Dynamic changes in the organophosphate profile upon treatment of the crystalline lens with dexamethasone. *Invest Ophthalmol Vis Sci* 23, 14-22.

67. Thomas D.M., Papadopoulou O., Mahenfroo P.P. and Zigman S. (1993) Phosphorus-31 NMR study of the effects of UV on squirrel lenses. *Exp Eye Res* 57, 59-65.

68. Lal S., Szwergold B.S., Taylor A.H., Randall W.C., Kappler F. and Brown T.R. (1995) Production of fructose and fructose 3-phosphate in maturing rat lenses. *Invest Ophthalmol Vis Sci* 36, 969-973.

69. Lal S., Szwergold B.S., Kappler F. and Brown T. (1993) Detection of fructose-3-phosphokinase activity in intact mammalian lenses by ^{31}P NMR spectroscopy. *J Biol Chem* 268, 7763-7767.

70. Greiner J.V., Kopp S.J. and Glonek T. (1985) Phosphorus nuclear magnetic resonance and ocular metabolism. *Surv Ophthalmol* 30, 189-202.

71. Nicholson J.K., Buckingham M.J. and Sadler P.J. (1983) High-resolution ^{1}H NMR studies of vertebrate blood and plasma. *Biochem J* 211, 605-615.

72. Bock J.L. (1982) Analysis of serum by high-field proton nuclear magnetic resonance. *Clin Chem* 28, 1873-1877.

73. Yoshikawa K., Matsushita K. and Ohsaka A. (1982) ^{1}H NMR spectroscopy in aqueous-media - examination of experimental conditions with human-urine as a model sample. *Physiol Chem Phys* 14, 385-389.

74. Nicholson J.K., Oflynn M.P., Sadler P.J., Macleod A.F., Juul S.M. and Sonksen P.H. (1984) Proton-nuclear-magnetic-resonance studies of serum, plasma and urine from fasting normal and diabetic subjects. *Biochem J* 217, 365-375.

75. Brown J.C.C., Sadler P.J., Spalton D.J., Juul S.M., Macleod A.F. and Sønksen P.H. (1986) Analysis of human aqueous humor by high-resolution ^{1}H NMR spectroscopy. *Exp Eye Res* 42, 357-362.

76. Gribbestad I. and Midelfart A. (1994) High-resolution ^{1}H NMR spectroscopy of aqueous humour from rabbits. *Graefe's Arch Clin Exp Ophthalmol* 232, 494-498.

77. Midelfart A., Dybdahl A. and Gribbestad I. (1996) Metabolic analysis of the rabbit cornea by proton nuclear magnetic resonance spectroscopy. *Ophthalmic Res* 28, 319-329.

78. Midelfart A., Dybdahl A. and Gribbestad S. (1996) Detection of different metabolites in the rabbit lens by high-resolution ^{1}H NMR spectroscopy. *Curr Eye Res* 15, 1175-1181.

79. Srivatsa G.S., M F C., D-S C. and B T. (1991) Detection and identification of endogenous small molecules in ocular tissues by proton nuclear magnetic resonance spectroscopy. *Curr Eye Res* 10, 127-132.

80. Midelfart A., Dybdahl A., Mueller N., Sitter B., Gribbestad I.S. and Krane J. (1998) Dexamethasone and dexamethasone phosphate detected by ^{1}H and ^{19}F NMR spectroscopy in the aqueous humour. *Exp Eye Res* 66, 327-337.

81. Midelfart A., Dybdahl A. and Krane J. (1999) Detection of dexamethasone in the cornea and lens by NMR spectroscopy. *Graefe's Arch Clin Exp Ophthalmol* 237, 415-423.

82. Pescosolido N., Miccheli A., Manetti C., Lannetti G.D., Feher J. and Cavallotti C. (2001) Metabolic changes in rabbit lens induced by treatment with dexamethasone. *Ophthalmic Res* 74, 68-74.

83. Bollard M.E., Garrod S., Holmes E., Lindon J.C., Humpfer E., Spraul M. and Nicholson J.K. (2000) High-resolution ^{1}H and ^{1}H-^{13}C magic angle spinning NMR spectroscopy of rat liver. *Magn Reson Med* 44, 201-207.

84. Cheng L.L., Chang I.W., Louis D.N. and Gonzalez R.G. (1998) Correlation of high-resolution magic angle spinning proton magnetic resonance spectroscopy with histopathology of intact human brain tumor specimens. *Cancer Res* 58, 1825-1832.

85. Griffin J.L., Troke J., Walker L.A., Shore R.F., Lindon J.C. and Nicholson J.K. (2000) The biochemical profile of rat testicular tissue as measured by magic angle spinning ^{1}H NMR spectroscopy. *FEBS Lett* 486, 225-229.

86. Sitter B., Bathen T., Hagen B., Arentz C., Skjeldestad F.E. and Gribbestad I.S. (2004) Cervical cancer tissue characterized by high-resolution magic angle spinning MR spectroscopy. *MAGMA* 16, 174-181.

87. Söderberg P.G., Chen E. and Lindström B. (1990) An objective and rapid method for determination of light dissemination in the lens. *Acta Ophthalmol (Copenh)* 68, 44-52.

88. Michael R., Söderberg P.G. and Chen E. (1998) Dose-response function for lens forward light scattering after in vivo exposure to ultraviolet radiation. *Graefe's Arch Clin Exp Ophthalmol* 236, 625-629.

89. Fan T.W.M. (1996) Metabolite profiling by one- and two-dimentional NMR analysis of complex mixtures. *Prog Nucl Magn Reson Spectr* 28, 161-219.

90. Willker W., Engelmann J., Brand A. and Liebfritz D. (1996) Metabolite identification in cell extracts and culture media by proton-detected 2D-H,C-NMR spectroscopy. *J Magn Reson Anal* 2, 21-32.

91. Gribbestad I.S., Petersen S.B., Fjösne H.E., Kvinnsland S. and Krane J. (1994) ^{1}H NMR Spectroscopic characterization of perchloric acid extracts from breast carcinomas and non-involved breast tissue. *NMR Biomed* 7, 181-194.

92. Le-Belle J.E., Harris N.G., Williams S.R. and Bhakoo K.K. (2002) A comparsion of cell and tissue extraction techniques using high-resolution ^{1}H-NMR spectroscopy. *NMR Biomed* 15, 37-44.

93. Sze D.Y. and Jardetzky O. (1990) Determination of metabolites and nucleotide concentrations in proliferating lymphocytes by ^{1}H-NMR of acid extracts. *Biochim Biophys Acta* 1054, 181-197.

94. Rujoi M., Jin J., Brochman D., Tang D. and Yappert C.M. (2003) Isolation and lipid characterizarion of cholesterol-enriched fractions in cortical and nuclear human lens fibres. *Invest Ophthalmol Vis Sci* 44, 1643-1642.

95. Yappert C.M., Rujoi M., Borchman D., Vorobyov I. and Estrada R. (2003) Glycero- versus sphingo-phospholipids: correlations with human and non-human mammalian lens growth. *Exp Eye Res* 76, 725-734.

96. Tofts P.S. and Wary S. (1988) A critical assessment of methods of measuring metabolite concenrations by NMR spectroscopy. *NMR Biomed* 1, 1-9.

97. Nicholson J.K. and Wilson I.D. (1989) High-resolution proton magnetic resonance spectroscopy of biological fluids. *Prog Nucl Magn Reson Spectr* 21, 449-501.

98. Kriat M., Confort-Gouny S., Vion-Dury J., Sciaky M., Viout P. and Cozzone P.J. (1992) Quantification of metabolites in human blood serum by proton magnetic resonace

spectroskopy. A comparative study of the use of formate and TSP as concentration standards. *NMR Biomed* 5, 179-184.

99. Becker E.D., Ferretti J.A. and Gambhir P.N. (1979) Selection of optimum parameters for pulse fourier transform nuclear magnetic resonance. *Anal Chem* 51, 1413-1420.

100. Cheng L.L., Ma M.L., Becerra L., Ptak T., Tracey I., Lackner A. and Gonzalez R.G. (1997) Quantitative neuropatology by high resolution magic angle spinning proton magnetic resonance spectroscopy. *Proc Nat Acad Sci USA* 94, 6408-6413.

101. Nicholson J.K. and Foxall J.D. (1995) 750 MHz ^{1}H and ^{1}H-^{13}C NMR spectroscopy of human blood plasma. *Anal Chem* 67, 793-811.

102. Lindon J.C., Nicholson J.K. and Everett J.R. (1999) NMR spectroscopy of biofluids. *Annu Rep NMR Spectros* 38, 1-88.

103. Behar K.L. and Ogino T. (1993) Characterization of macromolecule resonance in the ^{1}H NMR spectrum of rat brain. *Magn Reson Med* 30, 38-44.

104. Govindaraju V., Young K. and Maudsley A.A. (2000) Proton NMR chemical shifts and coupling constants for brain metabolites. *NMR Biomed* 13, 129-153.

105. Sze D.Y. and Jardetzky O. (1990) Characterization of lipid composition in simulated human lymphocytes by ^{1}H-NMR. *Biochim Biophys Acta* 1054, 198-206.

106. Wang Y. and Hollingsworth R.I. (1995) A solvent system for the high-resolution proton nuclear magnetic resonace spectrscopy of membrane lipids. *Anal Biochem* 225, 242-251.

107. Weybright P., Millis K., Campell N., Cory D.G. and Singer S. (1998) Gradient, high-resolution, magic angle spinning ^{1}H nuclear magneitc resonance spectroscopy of intact cells. *Magn Reson Med* 39, 337-344.

108. Podanyi B. and Reid S.R. (1988) NMR study of the conformations of free and lanthanide-complexed gluthatione in aqueous solution. *J Am Chem Soc* 110, 3805-3810.

109. Sze D.Y. and Jardetzky O. (1994) High-resolution proton NMR studies of lymphcyte extracts. *Immunometh* 4, 113-126.

110. Frantz A., Salla S. and Redbrake C. (1998) A sensitive assay for the quantification of glucose and lactate in the human cornea using a modified bioluminescence technique. *Graefe's Arch Clin Exp Ophthalmol* 236, 61-64.

111. Huxtable R.J. (1989) Taurine in the central nervous system and the mammalian actions of taurine. *Prog Neurobiol* 32, 471-533.

112. Pfister R.R., Nicolaro M.L. and Paterson C.A. (1981) Sodium citrate reduces the incidence of corneal ulcerations and perforations in extreme alkali-burned eyes - acetylcysteine and ascorbate have no favorable effect. *Invest Ophthalmol Vis Sci* 21, 486-490.

113. Mayr G.W. (1988) Inositol phosphates: structural components, regulators and signal transducers of the cell - a review. *Topics in Biochem* 7, 1-18.

114. Cammarata P.R., Zhou C., Chen G., Singh I., Reeves R.E., Kuszak J.R. and Robinson M.L. (1999) A transgenic animal model of osmotic cataract. Part 1: over-expression of biovine Na+/myo-inositol cotransporter in lens fibers. *Invest Ophthalmol Vis Sci* 40, 1727-1737.

115. Yokoyama T., Lin L.R., Bhargavan C. and Reddy V. (1993) Hypertonic stress increases NaK ATPase, taurine and myo-inositol in human lens and retinal pigment epithelial cultures. *Invest Ophthalmol Vis Sci* 34, 2512-2517.

116. Hightower K.R., Reddan J.R., McCready J.P. and Dziedzic D.C. (1994) Lens epithelium: a primary target of UVB irradiation. *Exp Eye Res* 56, 557-564.

117. Spector A. (1995) Oxidative stress-induced cataract: mechanism of action. *FASEB J* 9, 1173-1182.

118. Glonek T., Kopp S.J., Greiner J.V. and Sanders D.R. (1985) Lenticular energy metabolism during exogenous calcium deprivation and during recovery: effects of dextran-40. *Exp Eye Res* 40, 169-178.

119. Greiner J.V., Kopp S.J. and Glonek T. (1985) Phosphorus-31 NMR analysis of dynamic energy metabolism in intact crystalline lens treated with ouabain: phosphorylated metabolites. *Ophthalmic Res* 17, 269-278.

120. Greiner J.V., Kopp S.J., Sanders D.R. and Glonek T. (1982) Dynamic changes in the organophosphate profile of the experimental galactose-induced cataract. *Invest Ophthalmol Vis Sci* 22, 613-624.

121. Ayala M.N., Michael R. and Söderberg P.G. (2000) In vivo cataract after repeated exposure to ultraviolet radiation. *Exp Eye Res* 70, 451-456.

122. Shui Y.-B., Sasaki H., Pan J.-H., Hata I., Kojima M., Yamada Y., Hirai K.-I., Takahashia N. and Sasaki K. (2000) Morphological observation on cell death and phagocytosis induced by ultraviolet irradiation in a cultured human lens epithelial cell line. *Exp Eye Res* 71, 609-618.

123. Morán J., Hernández-Pech X., Merchant-Larios H. and Pasantes-Morales H. (2000) Release of taurine in apoptotic cerebellar granule neurons in culture. *Arc Eur J Physiol* 439, 271-277.

124. Desouky M.A., Geller A.M. and Jernigan H.M.J. (1992) Effect of osmotic stress on phosphorylcholine efflux and turnover in rat lenses. *Exp Eye Res* 54, 269-276.

125. Jernigan H.M.J., Desouky M.A., Geller A.M., Blum P.S. and Ekambaram M.C. (1993) Efflux and hydrolysis of phosphorylethanolamine and phosphorylcholine in stressed cultured rat lenses. *Exp Eye Res* 56, 25-33.

126. Miller T.J., Hanson R.D. and Yancey P.H. (2000) Developmental changes in organic osmolytes in prenatal and postnatal rat tissues. *Comp Biochem Physiol A* 125, 45-56.

127. Yancey P.H., Clark M.E., Hand S.C., Bowlus D.R. and Somero G.N. (1982) Living with water stress: evolution of osmolyte system. *Science* 217, 1214-1222.

128. Kador P.F., Akagi Y. and Kinoshita J.H. (1986) The Effect of aldose reductase and its inhibition on sugar cataract formation. *Metabolism* 35, 15-19.

129. van Heyningen R. (1959) Formation of polyols by the lens of the rat with "sugar" cataract. *Nature* 184, 194-195.

130. Malone J.I., Lowitt S. and Cook W.R. (1990) Nonosmotic diabetic cataracts. *Pediatr Res* 27, 293-296.

131. Obrosova I.G. and Stevens M.J. (1999) Effect of dietary taurine supplementation on GSH and NAD(P)-redox status, lipid peroxidation, and energy metabolism in diabetic precataractous lens. *Invest Ophthalmol Vis Sci* 40, 680-688.

132. Reeves R.E. and Cammarata P.R. (1996) Osmoregulatory alterations in myo-inositol uptake by bovine lens epithelial cells. Part 5. Mechanism of the myo-inositol efflux pathway. *Invest Ophthalmol Vis Sci* 37, 619-629.

133. Giblin F.J. (2000) Glutathione: a vital lens antioxidant. *J Ocul Pharmacol* 16, 121-135.

134. Gupta V. and Wagner B.J. (2003) Expression of the functional glucocorticoid receptor in mouse and human lens epithelial cells. *Invest Ophthalmol Vis Sci* 44, 2041-2046.

135. Dickerson J.E.J., Dotzel E. and Clark A.F. (1997) Steroid-induced cataract: new perspective from in vitro and lens culture studies. *Exp Eye Res* 65, 507-516.

136. Lindon J.C., Nicholson J.K., Holmes E. and Everett J.R. (2000) Metabonomics: metabolic processes studied by NMR spectroscopy of biofluids. *Concepts Magn Res* 12, 289-320.

137. Nicholson J.K., Connelly J., Lindon J.C. and Holmes E. (2002) Metabonomics: a platform for studying drug toxicity and gene function. *Nature reviews* 1, 153-161.

138. Wu K., Kojima M., Shui Y.B., Sasaki K. and Hockwin O. (1997) In vitro UVB effect on lens protein solutions. *Ophthalmic Res* 29, 75-82.

139. Takemoto L.J., Hansen J.S. and Horwitz J. (1983) Biochemical analysis of microdissected sections from the normal and cataractous human lens. *Curr Eye Res* 2, 443-450.

140. Müller A., Möller B., Dragomirescu V. and Hockwin O. (1987) Profiles of enzyme activities in bovine lenses (an application of a new slicing technique). *Concepts Toxicol* 4, 343-349.

141. Kojima M. (1990) Regional enzymatic analysis of UVB and streptozotocin induced diabetic cataract lens. *Lens Eye Toxic Res* 7, 547-561.

142. Rácz P., Hargitai C., Alföldy B., Bánki P. and Tompa K. (2000) ^{1}H spin-spin relaxation in normal and cataractous human, normal fish and bird eye lenses. *Exp Eye Res* 70, 529-536.

143. Neville M.C., Paterson C.A., Rae J.L. and Woessner D.E. (1974) Nuclear magnetic resonance studies and water "ordening" in the crytalline lens. *Science* 184, 1072-1074.

144. Wu J.C., Wong E.C., Arrindell E.L., Simons K.B., Jesmanowicz A. and Hyde J.S. (1993) In vivo determination of the anisotropic diffusion of water and the T_1 and T_2 times in the rabbit lens by high-resolution magnetic resonance imaging. *Invest Ophthalmol Vis Sci* 34, 2151-2158.

145. Moffat B.A. and Pope J.M. (2002) The interpretation of multi-exponential water proton transverse relaxation in the human and porcine eye lens. *Magn Reson Imag* 20, 83-93.

146. Moffat B.A., Landman K.A., Truscott R.J.W., Sweeney M.H.J. and Pope J.M. (1999) Age-related changes in the kinetics of water transport in normal human lenses. *Exp Eye Res* 69, 663-669.

147. Cheng H.-M., Kuan W.-P., Garrdio L. and Xiong J. (1992) High-resolution MR Imaging of water diffusion in the rabbit lens. *Exp Eye Res* 54, 127-132.

8. Appendices

Paper I

Is not included due to copyright

Paper II

Is not included due to copyright

Paper III

Time dependency of metabolic changes in rat lens after in vivo UVB irradiation analysed by HR-MAS ^{1}H NMR spectroscopy

Øystein Risa[1,3]
Oddbjørn Sæther[1,3]
Manoj Kakar[2]
Vino Mody[2]
Stefan Löfgren[2]
Per G. Söderberg[2]
Jostein Krane[1]
Anna Midelfart[3]

[1] Faculty of Natural Sciences and Technology, The Norwegian University of Science and Technology (NTNU), 7491 Trondheim, Norway

[2] St. Erik's Eye Hospital, Karolinska Institutet, SE-112 82 Stockholm, Sweden

[3] Faculty of Medicine, The Norwegian University of Science and Technology (NTNU), 7489 Trondheim, Norway

[1]Phone: +47 73 55 13 85
Fax: +47 73 59 12 83
Email: oystein.risa@biotech.ntnu.no

Abstract

Purpose: The lens ability to protect against, and repair ultraviolet radiation (UVR) induced damages, is of crucial importance to avoid cataract development. The influence of UVR-induced damage, and repair processes on the lens metabolites are not fully understood. Observation of short- and long-term changes in light scattering and the metabolic profile of pigmented rat lenses after threshold UVR exposure might serve to better understand the protective mechanisms in the lens. By using high resolution magic angle spinning (HR-MAS) ^{1}H NMR spectroscopy it was possible to investigate the metabolites of intact rat lenses.

Methods: Brown-Norway rats were exposed to 15 kJ/m^2 UVB irradiation. One eye was exposed and the contra lateral served as control. The rats were sacrificed 5, 25, 125, and 625 hrs post exposure and the lenses were removed. The degree of cataract was quantified by measurement of lens forward light scattering. Thereafter, proton NMR spectra from intact lenses were obtained and relative changes in metabolite concentrations were determined.

Results: The light scattering in the lens peaked at 25 hrs post-exposure and decreased thereafter. The lowest level of light scattering was measured 625 hrs after exposure. No significant changes in concentration were observed for the metabolites 5 and 25 hrs post-exposure except the total amount of adenosine tri- and diphosphate (ATP/ADP) that showed a significant decrease already 5 hrs after exposure. At 125 hrs the lens concentrations of lactate, succinate, phospho-choline, taurine, betaine, myo-inositol, and ATP/ADP showed a significant decrease ($p < 0.05$). Phenylalanine was the only metabolite that revealed a significant increase 125 hrs post exposure. At 625 hrs most of the metabolic changes seemed to normalise back to control levels. However, the concentration of betaine and phospho-choline were still showing a significant decrease 625 hrs after UVB irradiation.

Conclusion: The impact of UVB irradiation on the metabolic profile did not follow the same time dependency as the development of cataract. While the light scattering peaked at 25 hrs post-exposure, significant changes in the endogenous metabolites were observed after 125 hrs. Both the metabolic changes and the light scattering

seemed to average back to normal within a month after exposure. Significant decrease in osmolytes like taurine, myo-inositol and betaine indicated osmotic stress and loss of homeostasis. This study also demonstrated that HR-MAS ^{1}H NMR spectroscopy provides high quality spectra of intact lenses. These spectra contain a variety of information that might contribute to a better understanding of the metabolic response to drugs or endogenous stimuli like UVB irradiation.

1. Introduction

The cataractogenic effect of ultraviolet radiation (UVR) has been known since the beginning of the 20th century (Widmark, 1901). In addition, several epidemiological studies have implicated UVR as one of the environmental factors in human cataract formation (Zigman et al., 1979; Taylor et al., 1988; Cruickshanks et al., 1992; West et al., 1998). Considerable effort in clarifying the biochemical mechanisms in the lens tissue caused by UVR exposure has been undertaken, in hopes to avoid or delay the progression of lens opacification.

UVR damage in the lens is complex. Absorbed UVR photons excite lens molecules and create free radicals which increase the oxidative stress on the lens (Spector, 1995; Rose et al., 1998). This induces changes varying from modulated DNA syntesis (Andley et al., 1996), loss of ion homeostasis (Hightower et al., 1999) and accumulation of chromophores (Truscott et al., 1994; Dillon et al., 1999), to crystalline aggregation (Andley and Clark, 1989) and membrane damage (Kochevar, 1990; Hightower et al., 1994a). In the end UV irradiation might lead to epithelial cell death (Li and Spector, 1996; Michael et al., 1998a). Despite the impressive research effort the metabolic changes involved in these processes are by no means clear.

Severity of the lens damage is dependent on the UVR dose and it is assumed that UVR doses above a certain threshold level cause permanent damages to the lens (Pitts et al., 1977). Previous studies of lens damage after in vivo exposure to threshold doses of UVB irradiation (280 – 315 nm) found that the spatial organization of lens fibres was largely reversible eight weeks after (Michael et al., 2000). However, studies on morphological events alone are not enough to understand the biochemical mechanisms of the repairing processes. Ayala et al (Ayala et al., 2000) have suggested that opacities might develop due to an imbalance between damage and repair mechanisms in the lens. Results from our laboratory indicated that time dependent changes in the water soluble metabolites might differ from the light scattering changes in the lens caused by UVB irradiation (Risa et al., 2004). Investigation of the metabolic profile of the lens tissue under normal and cataractous conditions might contribute to our understanding of how the metabolism is influenced by UVB irradiation.

The aim of this study was to investigate the time dependency of metabolic changes after UVB irradiation by using nuclear magnetic resonance (NMR) spectroscopy.

During the last two decades NMR spectroscopy has proven to be a valuable tool for screening the metabolic profile in both tissue extracts and intact tissues. Thus, new bridges have been constructed between biochemistry and conventional histopathology (Lindon et al., 2003). Phosphorus-31 and proton NMR are the most common nuclei to be used in biological investigations. Several studies using ^{31}P or ^{1}H NMR spectroscopy have been performed on lens extracts (Meneses et al., 1990; Greiner et al., 1994; Midelfart et al., 1996; Risa et al., 2002).

Until recently only ^{31}P NMR spectroscopy has been found useful studying the metabolic profile of intact lens tissue (Greiner et al., 1981; Kopp et al., 1981). However, new approaches by using high resolution magic angle spinning (HR-MAS) NMR spectroscopy have made it possible to obtain high resolution ^{1}H NMR spectra of intact rat lens tissue (Risa et al., 2004). The principle of this method is that line broadening effects from dipolar couplings and chemical shift anisotropy are averaged to zero by rapid spinning of the sample (typically ~ 4–8kHz) at an angle of 54.7° relative to the static magnetic field (the magic angle). This non-destructive technique omits the time consuming extraction procedures that require relatively large amounts of tissue and might change the chemical composition of the samples. In comparison to ^{31}P NMR spectroscopy, HR-MAS ^{1}H NMR spectroscopy is more sensitive and can detect many more metabolites due to the natural abundance of proton in almost all metabolites.

In this study HR-MAS ^{1}H NMR spectroscopy was used to elucidate short- and long-term changes in the metabolic profile of pigmented rat lenses after moderate UVB irradiation. This might serve to a better understanding of the repairing mechanisms in the lens after UVR exposure.

2. Material & Methods

Animal experiments

Forty seven six-week-old Norwegian Brown rats were anesthetized with 45 mg/kg ketamine (Ketalar, Parke-Davis, Sweden) and 10 mg/kg xylazine (Rompun Vet., Bayer AB Sweden) intraperitoneally. Before irradiation pupils were dilated bilaterally with 1% tropicamide (Mydriacyl, Alcon Sverige AB, Sweden). After another 10 minutes, the eyes were unilaterally exposed to 15 kJ/m^2 UVB radiation, peak wavelength 302.6 nm, for 15 min. For more detailed description see Michael *et al* (Michael et al., 1996). The rats were sacrificed by CO_2 asphyxiation 5, 25, 125 and 625 hrs after UVB exposure. Both eyes were enucleated and the lenses were dissected free from remnants of ciliary body and zonular fibres. The isolated lenses were then put in room tempered Balanced Salt Solution (BSS, Alcon), photographed, and lens forward light scattering was quantified by the technique described previously (Söderberg et al., 1990). The samples were finally frozen and stored at -80°C before NMR spectroscopy. All animals were kept and treated according to the ARVO Statement for the Use of Animals in Ophthalmic and Vision Research.

NMR spectroscopy

HR-MAS ^1H NMR spectroscopy was performed on a BRUKER Avance DRX600 spectrometer (14.1 tesla, Bruker BioSpin GmbH, Germany) operating at 600 MHz for protons. The spectra were recorded at 4°C using a 4 mm HR-MAS $^1H/^{13}C$ probe. The temperature was calibrated using glucose as an internal thermometer (Nicholls and Mortishire-Smith, 2001). While still frozen, the lens sample was immersed in D_2O in a zirconium 4 mm diameter HR-MAS rotor (92 μl). Sodium-3'-trimethylsilylpropionate-2,2,3,3-d_4 (TSP) was used as an internal shift reference substance (0 ppm). Samples were spun at 5000 Hz.

Proton spectra were obtained using a one-dimensional T_2-fitered sequence [90°-(τ-180°- τ)$_n$-acquisition] (Carr-Purcell-Meiboom-Gill spin echo pulse sequence, CPMG) (Meiboom and Gill, 1958) to suppress signals from lipids and macromolecules. The inter pulse delay τ was 1 ms and the number of loops n was 72 (giving an effective echo time of 2nτ = 144 ms). Spectral region was 12 ppm with 32K data points. Acquisition time was 2.28 s and water presaturation was done with a selective pulse during a repetition delay of 3.1 s. Number of scans was 512. Zero-filling to 64K was

used and exponential line broadening of 1.0 Hz. For peak identification purposes, two-dimensional spectra such as gradient selected homo-nuclear shift correlated (gs-COSY) and J-resolved spectra were acquired, all under MAS conditions.
Analysis of the spectra was done with special software for analysis of complex mixtures (AMIX, Bruker BioSpin GmbH, Germany). The spectral region 0.8 – 10 ppm was reduced to a resolution of 0.001 ppm/point ('bucket' width). By performing a data reduction on the NMR spectra it was possible to summarize and compare sums of buckets over the exact same peak regions in each spectrum. The water peak between 6.3 and 4.7 ppm, and the region between 3.3 and 2.6 ppm, were eliminated from the data reduction. Peak areas were measured using the noise region (0.3 - 0.55 ppm) as an internal standard. The identity of samples during analysis was unknown to the spectroscopist.

Data analysis

Metabolite concentrations in the exposed groups were calculated relative to the levels in the control groups after normalization (integrated NMR peak/sample wet weight). The level of significance was set to 5%, and mean values were expressed with 95% confidence intervals.

3. Results

A significant increase ($p < 0.05$) in light scattering was observed for all UVB exposed lenses. The lens light scattering peaked at 25 hrs post-exposure and decreased thereafter (Fig. 1). The lowest level of light scattering was measured 625 hrs after exposure.

The HR-MAS ^{1}H NMR spectra obtained from intact rat lenses were of high resolution quality comparable to those obtained in previous experiments with intact lens tissue (Risa et al., 2004) and tissue extracts (Risa et al., 2002). A representative reduced NMR spectrum (bucket width 0.001 ppm) of a control lens with peak assignments of more than 25 different metabolites is presented in Fig. 2. Due to overlap and insufficient signal-to-noise ratio, some of the assigned metabolites could not be quantified. Fourteen different metabolites were found suitable for quantitative analysis. These were lactate, taurine, myo-inositol, betaine, phospho-choline (p-choline), reduced glutathione (GSH), succinate, glycine, glutamate, tyrosine, valine, alanine, phenylalanine, and the total amount of adenosine tri- and diphosphate (ATP/ADP). The measured peak regions for the respective metabolites are illustrated as dark areas in Fig. 2.

Mean values of the relative concentration differences of the metabolites between exposed and non-exposed lenses were calculated at 5, 25, 125, and 625 hrs post-exposure. The results are given in Fig. 3. As shown in this figure no significant changes in concentration were observed for all metabolites at 5 and 25 hrs post-exposure with exception of ATP/ADP showing a significant decrease already 5 hrs after exposure. At 125 hrs, the lens concentrations of lactate, succinate, p-choline, taurine, betaine, myo-inositol, and ATP/ADP showed a significant decrease ($p < 0.05$). The same tendency was observed for glycine and GSH but without reaching a significant level. Valine, alanine and phenylalanine peaked at 125 hrs, with phenylalanine increasing significantly. Tyrosine concentration was lightly increased at all post exposure observation points ($p > 0.05$). The concentration of glutamate had an indicative peak at 25 hrs post-exposure, but the following changes were not significantly different from controls for any of the observed time-points after UVB irradiation. At 625 hrs most of the metabolic changes seemed to normalise back to near-control values. However, the concentrations of betaine and p-choline were still showing a significant decrease 625 hrs after UVB irradiation.

4. Discussion

As shown recently in our laboratory, HR-MAS ^{1}H NMR spectroscopy has a great potential in analysing the metabolic profile of intact lens tissues (Risa et al., 2004). The detailed information on the metabolic composition was comparable to that acquired by NMR spectroscopy of lens tissue extracts (Midelfart et al., 1996; Risa et al., 2002). In the present study broad resonances from macromolecules and lipids with low mobility and hence short transverse relaxation time (T_2) were suppressed by using a one dimensional T_2-filtered pulse sequence with an effective spin echo delay of 144 ms. This allowed an enhancement in relative signal intensity of smaller molecules and better baseline separation of the peaks. However, as explained by Risa et al (Risa et al., 2004) it was difficult to use conventional quantification methods with TSP as internal standard. By analysing the samples under identical conditions and assuming that each metabolite had the same T_2 in all samples, this problem was avoided by measuring peak intensities relative to a selected noise region and correcting for the lens wet weight. Relative changes could then be extracted.

The metabolic profile of the pigmented rat lens in this study was very similar to previous HR-MAS studies of albino Sprague Dawley rats of the same age (Risa et al., 2004). The same metabolites dominated the one-dimensional proton spectra, and the same cross-peaks were revealed in the assignment work of the two-dimensional spectra. However, a comparative study of the metabolic profile of lenses from pigmented and albino rat eyes were not performed.

The observed increase in light scattering from the lens after UVB irradiation was transient, showing a maximum at 25 hrs post exposure. The decrease in light scattering between 25 and 625 hrs latency showed that 15 kJ/m^2 is below or close-to-threshold dose for the pigmented rat lens (Pitts et al., 1977; Michael et al., 1996). Comparing the light scattering differences and changes of the metabolic profile in the lens, the impact of the UVB irradiation on the metabolite processes seemed to be delayed. This because the major changes in the metabolite concentration were observed first at 125 hrs post exposure. Similar to the normalisation of light scattering, the concentrations of most of the metabolites seemed to converge back to the normal level after 625 hrs.

In earlier studies, different time intervals for repeated threshold doses of UVB irradiation have shown that the most severe cataract development occurred in a group that was allowed a 72 hrs interval between two exposures. In contrast to that,

the damage was the same whether the second exposure was repeated immediately, 6 hrs or 24 hrs after. The lowest intensity of light scattering was detected in the 30 days interval group (Ayala et al., 2000). It was suggested that photoproduct formation, different repair mechanisms and apoptosis might make the lens cells more sensitive to a second UVB exposure. In the present work, the peak change in the endogenous metabolite concentrations at 125 hrs post exposure supports the observations that the lens is vulnerable to additional UVB attacks at certain time intervals. The normalization of the metabolic changes after 625 hrs (26 days) indicates however, that the biochemical repair in the lens can occur within a month after irradiation. Consequently when repeated UVB exposures are separated by 30 days, the final damage of the lens might be less than with shorter time intervals.
Both taurine and myo-inositol are among the organic osmolytes that have been previously identified in the lens (Miller et al., 2000; Cammarata et al., 2002) and their significant decrease 125 hrs post exposure might be explained by changes in epithelial membrane permeability, osmotic stress and loss of homeostasis (Hightower et al., 1994b). Michael et al (Michael et al., 1998a) have observed that threshold UVB irradiation induced apoptosis in the lens epithelial cells leading to loss of metabolically competent cells and disturbance of the water balance in the lens. Taurine is released in association with cell shrinkage and water extrusion during apoptosis in neurons (Morán et al., 2000). The observed decrease in taurine and myo-inositol indicates a possible relationship between apoptosis and extrusion of organic osmolytes in rat lens after UVB irradiation. Also the level of betaine, known as a dominating osmolyte in placenta and renal medulla tissue (Miller et al., 2000), fell significantly 125 hrs post exposure. So far, no osmolytic activity has been reported for betaine in the lens (Miller et al., 2000). In fact the lenticular role of betaine is not exactly known (Rao et al., 1998). Some osmolytes, especially methylamines like betaine, may have stabilising effects on macromolecules (Yancey et al., 1982). This effect is of crucial importance to the lens fibre cells which have limited capacity of damage repair (Spector, 1995).
The phospholipid precursor p-choline is one of the most abundant metabolites in the rat lens and an important metabolite in cell membrane metabolism (Kopp et al., 1981). Studies have shown that cataractogenic osmotic and oxidative stress caused an increased efflux of lenticular organic phosphate compounds, including p-choline (Desouky et al., 1992; Jernigan et al., 1993). Investigation of apoptotic cell death in

lymphoblast has revealed a decrease in p-choline during the cytoskeletal architectural destruction, and suggested that small molecules like p-choline may not be replenished as the cell prepares to die {Blankenberg *et al.*, 1997}}. In agreement with earlier observations on osmotic stressed rat lenses (Jernigan et al., 1993), present study observed a time dependent reduction in lenticular p-choline after UVB irradiation.

The delayed time response of the observed concentration changes indicate that initial changes in the lens epithelium (Li and Spector, 1996; Shui et al., 2000) might induce additional biochemical changes in the bulk of the lens at a later stage. Indeed it has been suggested that many of the damages associated with cataract such as Na/K-ATPase inhibition, drop in GSH concentration, loss of ATP, changes in water balance and lens protein modifications are all potential results of early changes in the epithelial cells and might occur in a post-insult period 1-12 days later (Hightower and McCready, 1992; Li et al., 1995). Histological analysis of albino rat lenses showed that severe damages in underlying fibre cells did not appear until seven days after threshold UVB exposure (Michael et al., 1998a). In present study threshold UVB doses was found to cause significant post-insult disturbances as late as 125 hrs after irradiation, starting thereafter the repair process with normalization of the metabolism. It has been suggested that polymerization of crystalline cleavage products causes the formation of water-insoluble polypeptides in the lens (Srivastava, 1988; Baruch et al., 2001). Therefore, proteases that further degrade the protein fragments into smaller peptides and amino acids might provide an important secondary defence against aggregation and cataract development (Taylor and Davies, 1987; Chaerkady and Sharma, 2004). The significant increase of phenylalanine and the increasing tendency of valine and alanine ($p > 0.05$) might be due to induction of site specific hydrolysis of multicatalytic proteases.

Glutathione (GSH) has an important role in protecting protein thiol-groups from oxidative damage and preventing cross-linking of soluble crystallines (Reddy, 1990). GSH concentration has showed a rapid depletion in lens epithelium and more slowly in the underlying lens fibres after UVB irradiation (Hightower and McCready, 1992). However, the lens epithelial cells have a remarkable ability to re-establish GSH to a normal level (Spector, 1995). The present findings of unchanged GSH level in the post irradiation period from 5 to 625 hrs indicated that the lens maintained a vital GSH metabolism.

Normal GSH turnover in the lens requires high amount of energy (Reddy, 1990), which might be one the reasons for the significant reduction in ATP and ADP level post irradiation. In general, repair processes results in increased energy demand and as shown previously photochemical stress induces a decrease in the ATP level (Thomas et al., 1993; Spector, 1995).

The ATP production in the lens continues even after severe epithelial damage (Spector, 1995). This is because the bulk of the lens relies on anaerobic glycolysis, represented throughout the lens, with lactate as the end product catalyzed by lactate dehydrogenase (LDH). Löfgren and Söderberg have reported that UVB irradiation inhibits the activity of LDH in the lens, and this might lead to energy depletion (Löfgren and Söderberg, 2001). The significant decrease in both lactate and ATP/ADP observed at 125 hrs post exposure supports these observations.

Potential local variations in lens nucleus, cortex and epithelium were not addressed in the present study. HR-MAS ^{1}H NMR spectroscopy has the potential to investigating the metabolic profile of very small lenticular sections. Thus, in further studies it might be possible to investigate separately local metabolic changes in the anterior, nuclear and posterior sections of the rat lens.

In summary this study showed that the UVB irradiation impact on the metabolic profile of rat lens did not follow the same time relationship as the development of light scattering. While the light scattering peaked at 25 hrs post exposure, most significant changes in the endogenous metabolites were observed after 125 hrs. Both the metabolic changes and the light scattering seemed to average back to normal within a month after exposure. Most of the observed changes were concentration decrease of several water soluble metabolites, similar to earlier observations in albino lenses (Risa et al., 2004). Significant decrease in osmolytes like taurine, myo-inositol and betaine indicated a loss of homeostasis and osmotic stress. Our laboratory is the first to report a biological response of betaine metabolism in the lens. This study also demonstrates that HR-MAS ^{1}H NMR spectroscopy provided high quality spectra of intact lens tissue and a large number of water soluble metabolites could be directly investigated. The results might contribute to a better understanding of the metabolic response to external pathophysiological stimuli like UVB irradiation.

Acknowledgements

This study was supported by grants from Health and Rehabilitation, Norway.

References

Andley U.P., Clark B.A., 1989. The effects of near-UV radiation on human lens crystallins: proteins structural changes and the production of O_{2^-} and H_2O_2 . Photochem. Photobiol. 50, 97-105.

Andley U.P., Fritz C., Morrison A.R., Becker B., 1996. The role of prostaglandins E2 and F2 alpha in ultraviolet radiation-induced cortical cataracts in vivo. Invest. Ophthalmol. Vis. Sci. 37, 1539-1548.

Ayala M.N., Michael R., Söderberg P.G., 2000. In vivo cataract after repeated exposure to ultraviolet radiation. Exp. Eye Res. 70, 451-456.

Baruch A., Greenbaum D., Levy E.T., Nielsen P.A., Gilula N.B., Kumar N.M., Bogyo M., 2001. Defining a link between gap junction communication, proteolysis, and cataract formation. J. Biol. Chem. 276, 28999-29006.

Cammarata P.R., Schafer G., Chen S.W., Guo Z. and Reeves R.E., 2002. Osmoregulatory alterations in taurine uptake by cultured human and bovine lens epithelial cells. Invest. Ophthalmol. Vis. Sci. 43, 425-433.

Chaerkady R., Sharma K.K., 2004. Characterization of a bradykinin-hydrolyzing protease from the bovine lens. Invest. Ophthalmol. Vis. Sci. 45, 1214-1223.

Cruickshanks K.J., Klein B.E., Klein R., 1992. Ultraviolet light exposure and lens opacities: the Beaver dam eye study. Am. J. Public. Health. 82, 1658-1662.

Desouky M.A., Geller A.M., Jernigan H.M.J., 1992. Effect of osmotic stress on phosphorylcholine efflux and turnover in rat lenses. Exp. Eye Res. 54, 269-276.

Dillon J., Ortwerth B.J., Chingnell C.F., Reszka K.J., 1999. Electron paramgnetic resonance and spin trapping investigations of the photoreactivity of human lens proteins. Photochem. Photobiol. 69, 259-264.

Greiner J.V., Auerbach D.B., Leahy C.D., Gloneck T., 1994. Distribution of membrane phospholipids in the crystalline lens. Invest. Ophthalmol. Vis. Sci. 35, 3739-3746.

Greiner J.V., Kopp S.J., Sanders D.R., Glonek T., 1981. Organophosphates of the crystalline lens: a nuclear magnetic resonance spectroscopic study. Invest. Ophthalmol. Vis. Sci. 21, 700-713.

Hightower K., McCready J., 1992. Mechanisms involved in cataract development following near-ultraviolet radiation of cultured lenses. Curr. Eye Res. 11, 679-689.

Hightower K.R., Duncan G., Dawson A., Wormstone I.M., Reddan J., Dziedizc D., 1999. Ultraviolet irradiation (UVB) interrupts calcium cell signaling in lens epithelial cells. Photochem. Photobiol. 69, 595-598.

Hightower K.R., McCready J.P., Brochman D., 1994a. Membrane damage in UVB irradiated lenses. Photochem. Photobiol. 59, 485-490.

Hightower K.R., Reddan J.R., McCready J.P., Dziedzic D.C., 1994b. Lens epithelium: a primary target of UVB irradiation. Exp. Eye Res. 56, 557-564.

Jernigan H.M.J., Desouky M.A., Geller A.M., Blum P.S., Ekambaram M.C., 1993. Efflux and hydrolysis of phosphorylethanolamine and phosphorylcholine in stressed cultured rat lenses. Exp. Eye Res. 56, 25-33.

Kochevar I.E., 1990. UV-induced protein alterations and lipid oxidation in erytrocyte membranes. Photochem. Photobiol. 52, 795-800.

Kopp S.I., Greiner J.V., Glonek T., 1981. Analysis of intact rat lens metabolites by P-31 NMR spectroscopy. Curr. Eye Res. 1, 375-381.

Li W.-C., Kuszak J.R., Dunn K., Wang R.-R., Ma W., Wang G.-M., Spector A., Lieb M., Cotliar A.M., Weiss M., Espy J., Howard G., Farris R.L., Auran J., Donn A., Hofeldt A., Mackay C., Merriam J., Mittl R., Smith T.R., 1995. Lens epithelial cell apoptosis appears to be a common cellular basis for non-cogenital cataract development in humans and animals. J. Cell Biol. 130, 169-181.

Li W.-C., Spector A., 1996. Lens epithelial cell apoptosis is an early event in the development of UVB-induced cataract. Free Radic. Biol. Med. 20, 301-311.

Lindon J.C., Holmes E., Nicholson J.K., 2003. So what's the deal with metabonomics. Anal. Chem. 75, 384A-391A.

Löfgren S., Söderberg P.G., 2001. Lens lactate dehydrogenase inactivation after UV-B irradiation: an in vivo measure of UVR-B penetration. Invest. Ophthalmol. Vis. Sci. 42, 1833-1836.

Meiboom S., Gill D., 1958. Modified spin-echo method for measuring nuclear relaxation times*. The Review of Scientific Instruments 29, 688-691.

Meneses P., Greiner J.V., Glonek T., 1990. Comparsion of membrane phospholipids of the rabbit and pig crystalline Lens. Exp. Eye Res. 50, 235-240.

Michael R., Vrensen G.F.J.M., Marle J.v., Gan L., Söderberg P.G., 1998a. Apoptosis in the rat lens after in vivo threshold dose ultraviolet irradiation. Invest. Ophthalmol. Vis. Sci. 39, 2681-2687.

Michael R., Söderberg P.G., Chen E., 1996. Long-term development of lens opacities after exposure to ultraviolet radiation at 300 nm. Ophthal. Res. 28, 209-218.

Michael R., Söderberg P.G., Chen E., 1998b. Dose-response function for lens forward light scattering after in vivo exposure to ultraviolet radiation. Graefe's Arch. Clin. Exp. Ophthalmol. 236, 625-629.

Michael R., Vrensen G.F.J.M., Marle J.v., Löfgren S., Söderberg P.G., 2000. Repair in the rat lens after threshold ultraviolet radiation injury. Invest. Ophthalmol. and Vis. Sci. 41, 204-212.

Midelfart A., Dybdahl A., Gribbestad S., 1996. Detection of different metabolites in the rabbit lens by high resolution 1H NMR spectroscopy. Curr. Eye Res. 15, 1175-1181.

Miller T.J., Hanson R.D., Yancey P.H., 2000. Developmental changes in organic osmolytes in prenatal and postnatal rat tissues. Comp. Biochem. Physiol. A 125, 45-56.

Morán J., Hernández-Pech X., Merchant-Larios H., Pasantes-Morales H., 2000. Release of taurine in apoptotic cerebellar granule neurons in culture. Pflüger's Arc. – Eur. J. Physiol. 439, 271-277.

Nicholls A.W., Mortishire-Smith R.J., 2001. Temperature calibration of a high-resolution magic-angle spinning NMR probe for analysis of tissue samples. Magnet. Reson. Chem. 39, 773-776.

Pitts D.G., Cullen A.P., Hacker P.D., 1977. Ocular effects of ultraviolet radiation from 295 to 365 nm. Invest. Ophthalmol. Vis. Sci. 16, 932-939.

Rao P.V., Garrow T.A., John F., Garland D., Milland N.S., Zigler J.S.J., 1998. Betaine-homocysteine Methyltransferase Is a Developmentally Regulated Enzyme Crystallin in Rhesus Monkey Lens. J. Biol. Chem. 273, 30669-30674.

Reddy V.N., 1990. Glutathione and its Function in the Lens - An Overview. Exp Eye Res 50, 771-778.

Risa Ø., Sæther O., Löfgren S., Söderberg P.G., Krane J., Midelfart A., 2004. Metabolic changes in rat lens after in vivo exposure to ultraviolet irradiation: measurements by high resolution MAS ^{1}H NMR spectroscopy. Invest. Ophthalmol. Vis. Sci. 45, 1916-1921.

Risa Ø., Sæther O., Midelfart A., Krane J., Cejkova J., 2002. Analysis of immediate changes of water-soluble metabolites in alkali-burned rabbit cornea, aqueous humor and lens by high-resolution ^{1}H-NMR spectroscopy. Graefe's Arch. Clin. Exp. Ophthalmol. 240, 49-55.

Rose R.C., Richer S.P., Bode A.M., 1998. Ocular oxidants and antioxidant protection [review]. Proc. Soc. Exp. Biol. Med. 217, 397-407.

Shui Y.-B., Sasaki H., Pan J.-H., Hata I., Kojima M., Yamada Y., Hirai K.-I., Takahashia N., Sasaki K., 2000. Morphological observation on cell death and phagocytosis induced by ultraviolet irradiation in a cultured human lens epithelial cell line. Exp. Eye Res. 71, 609-618.

Spector A., 1995. Oxidative stress-induced cataract: mechanism of action. FASEB J 9, 1173-1182.

Srivastava O.P., 1988. Age-related increase in concentration and aggregation of degraded polypeptides in human lenses. Exp. Eye Res. 47, 525-543.

Söderberg P.G., Chen E., Lindström B., 1990. An objective and rapid method for determination of light dissemination in the lens. Acta Ophthalmol. (Copenh) 68, 44-52.

Taylor A., Davies K.J.A., 1987. Protein oxidation and loss of protease activity may lead to cataract formation in the aged lens. Free Radic. Biol. Med. 3, 371-377.

Taylor H.R., West S.K., Rosenthal F.S., Munoz B., Newland H.S., Abbey H., Emmet E.A., 1988. Effect of ultraviolet radiation in cataract formation. N. Engl. J. Med. 319, 1429-1433.

Thomas D.M., Papadopoulou O., Mahendroo P.P., Zigman S., 1993 P-31 NMR-study of the effects of UV on squirrel lenses. Exp. Eye Res. 57, 59-65.

Truscott R.J.W., Wood A.M., Carver J.A., Sheil M.M., Stutchbury G.M., Zhu J., Kilby W., 1994. A new UV-filter compuond in human lenses. FEBS Lett. 348, 173-176.

West S.K., Duncan D.D., Munoz B., Rubin G.S., Fried L.P., Bandeen-Roche K., Schein O.D., 1998. Sunlight exposure and risk of lens opacities in a population-based study: the Salisbury eye evaluation project. JAMA. 280, 714-718.

Widmark J. (1901) Über den einfluss des lichtes auf die linse. Mitteil. Augenklin. Carol. Med. Chir. Inst. Stockholm 3, 125-149.

Yancey P.H., Clark M.E., Hand S.C., Bowlus D.R., Somero G.N., 1982. Living with water stress: evolution of osmolyte system. Science. 217, 1214-1222.

Zigman S., Datiles M., Torczynski E., 1979. Sunlight and human cataracts. Invest. Ophthalmol. Vis. Sci. 18, 462-467.

Figure Legends

Fig. 1. Difference in intensity of forward light-scattering between exposed and non-exposed rat lenses 5 (n = 12), 25 (n = 12), 125 (n = 12) and 625 (n = 11) hrs after UVB irradiation. The UVRB dose was 15 kJ/m^2. The bars represent 95% confidence intervals for the paired-sample mean differences. $_t$EDC represents the transformed equivalent diazepam concentration. (Michael et al., 1998b)

Fig. 2. A representative HR-MAS ^{1}H NMR spin-echo spectrum of an intact rat lens (control), reduced by the software AMIX, Bruker BioSpin to a resolution of 0.001 ppm/point ('bucket' width). The dark regions represent the integrated area of the respective metabolites analysed. **(A)** High field, **(B)** middle field and **(C)** low field region of the obtained spectrum. The ppm values were assigned using TSP as reference substance at 0 ppm. Assignments: GSH, reduced glutathione; NAD/NADH, nicotine adenine dinucleotide; ATP/ADP/AMP, adenosine tri-/di-/monophosphate; UTP/UDP, uridine tri-/diphosphate.

Fig. 3. Relative differences in metabolite concentrations between exposed and non-exposed rat lenses 5 (n = 6), 25 (n = 6), 125 (n = 7) and 625 (n = 6) hrs after UVB irradiation. Data were calculated as (exposed lens – control lens)/control lens. The bars represent 95% confidence intervals for the mean differences.

Figure 1.

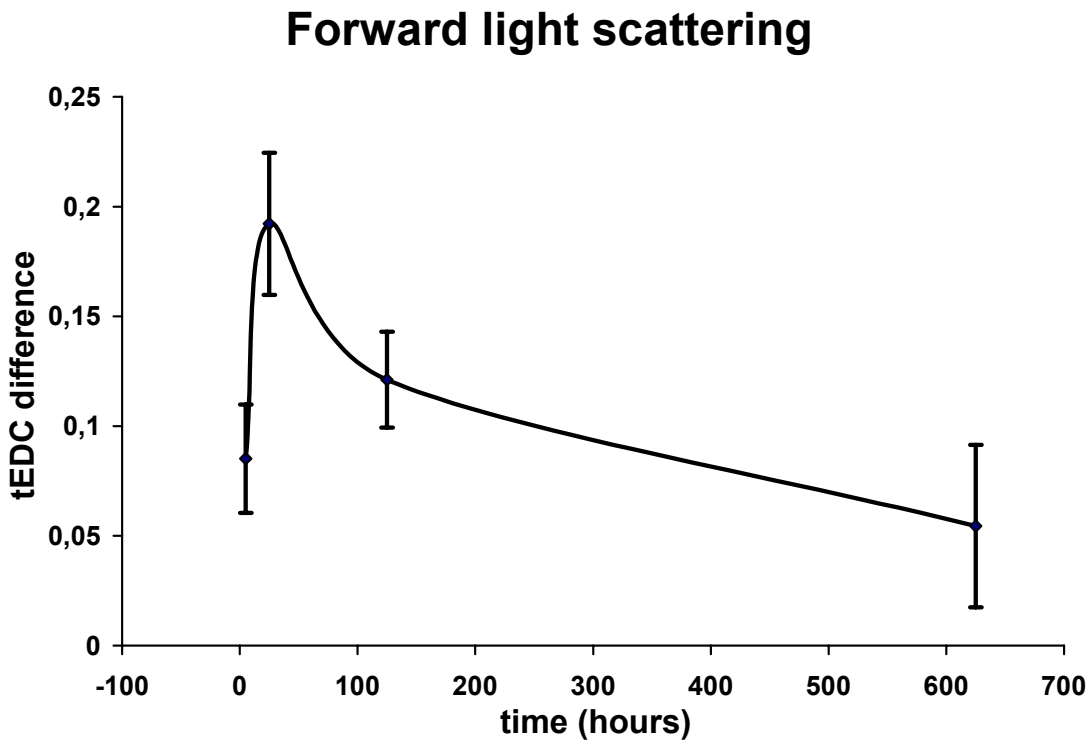
Forward light scattering
tEDC difference
0,25
0,2
0,15
0,1
0,05
0
-100
0
100
200
300
400
500
600
700
time (hours)

Figure 2.

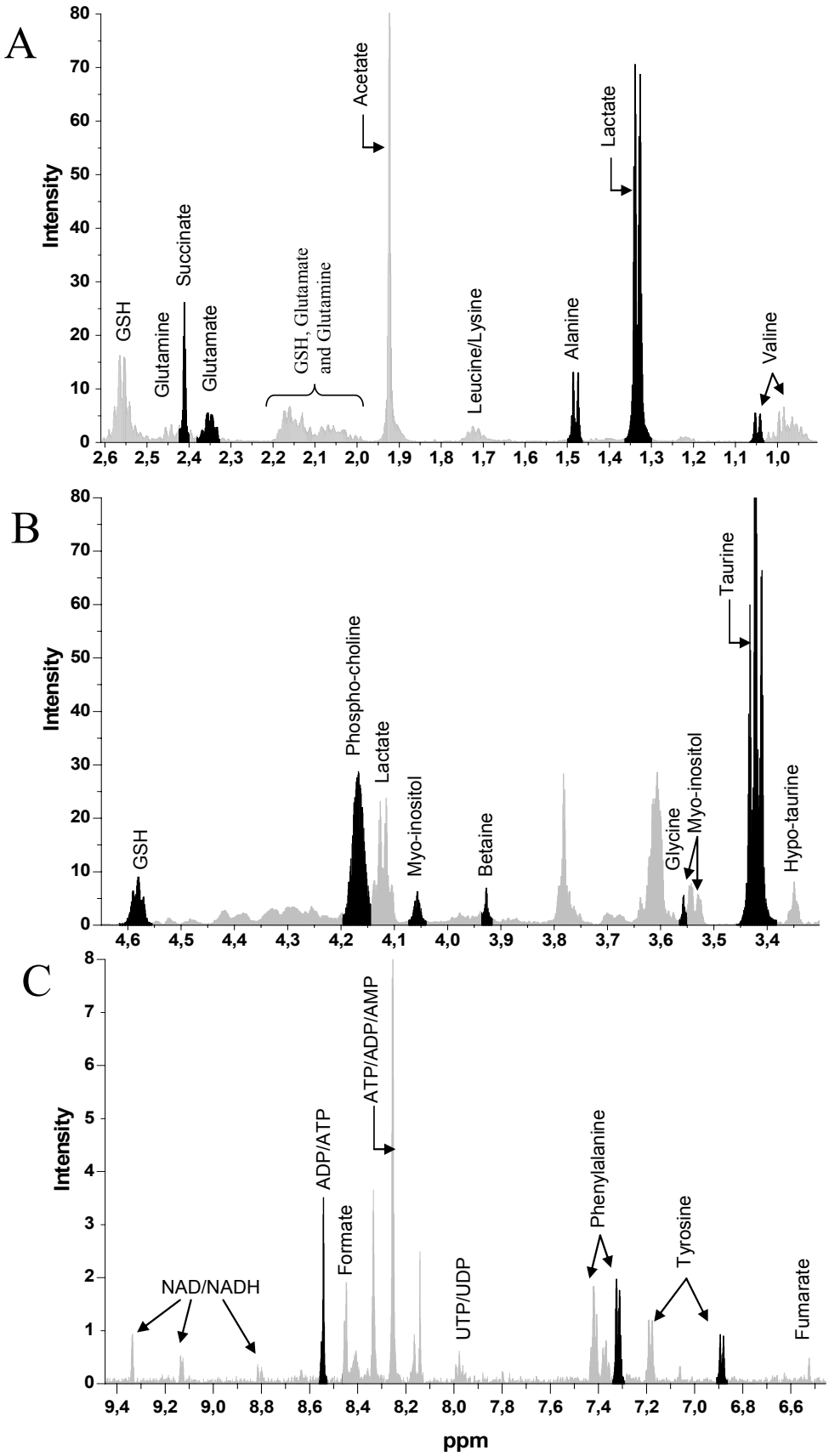
A
Intensity
GSH
Glutamine
Succinate
Glutamate
GSH, Glutamate and Glutamine
Acetate
Leucine/Lysine
Alanine
Lactate
Valine
B
Intensity
GSH
Phospho-choline
Lactate
Myo-inositol
Betaine
Glycine
Myo-inositol
Taurine
Hypo-taurine
C
Intensity
NAD/NADH
ADP/ATP
Formate
ATP/ADP/AMP
UTP/UDP
Phenylalanine
Tyrosine
Fumarate
ppm

Figure 3.

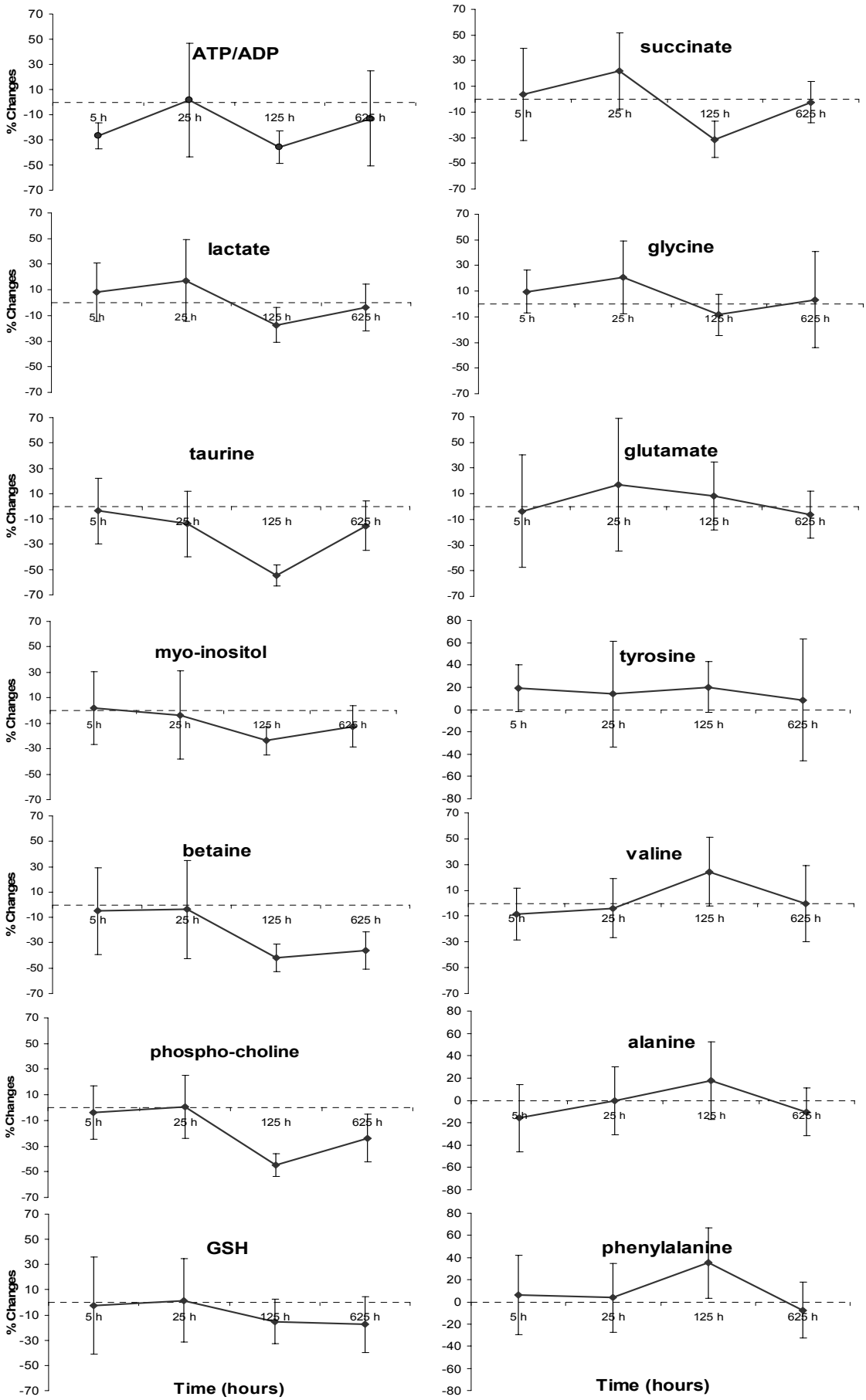
ATP/ADP
succinate
lactate
glycine
taurine
glutamate
myo-inositol
tyrosine
betaine
valine
phospho-choline
alanine
GSH
phenylalanine
% Changes
5 h
25 h
125 h
625 h
Time (hours)

Paper IV

High-Resolution Magic Angle Spinning ^{1}H NMR Spectroscopy of Metabolic Changes in Rabbit Lens after Treatment with Dexamethasone Combined with UVB Exposure

List of authors:

Oddbjørn Sæther[1, 2]
Øystein Risa[1, 2]
Jitka Čejková[3]
Jostein Krane[2]
Anna Midelfart[1]

[1] Faculty of Medicine, Norwegian University of Science and Technology (NTNU), Trondheim, Norway
[2] Faculty of Natural Sciences and Technology, Norwegian University of Science and Technology (NTNU), Trondheim, Norway
[3] Department of Eye Histochemistry and Pharmacology, Institute of Experimental Medicine, Academy of Sciences of the Czech Republic, Prague, Czech Republic

Corresponding author's address:
Oddbjørn Sæther
MR-Senteret
St. Olavs Hospital
7006 Trondheim, Norway
Tel.: +47 73 86 76 70
Fax: +47 73 86 77 08
e-mail: Oddbjorn.Sather@medisin.ntnu.no

Abstract

Background

Long-term steroid treatment and UVB exposure are well known cataractogenic factors. The purpose of this study was to investigate metabolic changes in the rabbit lens after long-term dexamethasone treatment in combination with UVB exposure, using High-Resolution Magic Angle Spinning Proton Nuclear Magnetic Resonance (HR-MAS ^{1}H NMR) Spectroscopy to analyse intact lens tissues.

Methods

Rabbits received topical doses of 0.1% dexamethasone or 0.9% saline (50 μl) four times daily during 36 days. On day 37, the eyes were exposed to UVB radiation (2.05 J/cm^{2}). Twenty-four hours later the animals were sacrificed, and HR-MAS ^{1}H NMR spectra of lens tissues were obtained.

Results

More than 15 major metabolites were assigned in NMR spectra of rabbit lenses. The combined treatment with dexamethasone and UVB induced large reductions in the concentration of GSH, inositols, taurine and lactate, as compared to normal lens. Concurrently, the levels of glucose, sorbitol and sorbitol-3-phosphate were increased. After exposure to UVB radiation only, the most significant result was a decrease in the concentration of lactate. No lens opacities were detected.

Conclusions

HR-MAS ^{1}H NMR spectroscopy was found to be an efficient tool for analysis of intact lens tissues. High-resolution NMR spectra of intact lens tissue enabled metabolic changes to be quantified. Long-term treatment with dexamethasone combined with UVB exposure induced substantial metabolic changes, dominated by osmolytic regulation processes and loss of glutathione.

Introduction

Cataract formation is a well-established side effect of long-term treatment with glucocorticoids [39]. However, the exact mechanism of steroid-induced cataract is not known [15]. Biochemical changes such as the occurrence of glucocorticoid-protein adducts [2] and loss of glutathione [42] have been observed within the lens in animal experiments. From human lens protein culture studies, formation of disulfide-linked protein aggregates have been reported following steroid treatment [3].

Cataract is a multifactorial process, so it may not be sufficient to test the lenticular metabolic effect of a drug alone. Instead, different cataractogenic factors should be combined [44] due to their additive or even synergistic effects [39]. Among others, ultraviolet B (UVB) radiation is a risk factor for the development of cataract [45]. In the rabbit lens, cataract develops following relatively low-level UVB irradiation (1-2 mW/cm^2) [16]. Thus, exposition to UVB radiation might enhance development of cataract induced by steroids.

By the application of NMR (nuclear magnetic resonance) spectroscopy on biological samples, numerous metabolites can be monitored simultaneously. Metabolic changes in the rabbit lens after treatment with steroids like dexamethasone have previously been investigated by NMR spectroscopy, i.e. organophosphate profiling of incubated lenses and their extracts [13] and analysis of lens extracts after long-term topical treatment [31]. In our laboratory, ^{19}F and ^{1}H NMR spectroscopy have been applied to monitor penetration of dexamethasone into the anterior segment of the eye after short-term topical treatment, analysing tissue extracts from cornea and lens [27]. However, tissue extraction procedures involve extensive treatment of the samples, which might change their biochemical composition. Also, a relatively large amount of tissue is required. Thus, analysis of intact tissue samples is preferable. Such opportunity is provided by the application of high-resolution magic angle spinning (HR-MAS) NMR spectroscopy. Using this technique, peak broadening effects caused by anisotropic interactions are averaged to zero by fast spinning of the sample at a certain angle (54.7°) between the spinning axis and the static magnetic field. As shown previously with other tissues [1, 4, 5, 28], spectral resolution comparable to

those obtained from liquid extracts can be achieved by means of HR-MAS ^{1}H NMR spectroscopy.

The purpose of this study was to investigate metabolic changes in the rabbit lens after combined treatment with dexamethasone and UVB exposure, using HR-MAS ^{1}H NMR spectroscopy to analyse intact lens tissues. The feasibility of HR-MAS ^{1}H NMR spectroscopy of intact lens tissue will be discussed.

Materials and methods

Animal experiments

Albino rabbits (New Zealand white, body weight 2.5-3.0 kg) were divided into three groups. In the first group both eyes of four rabbits were topically treated with 0.1% dexamethasone (Decadron, Merck, Sharp & Dohme, Whitehouse Station, NJ, USA) before exposure to UVB radiation (dxm/UVB group). In the second group three rabbits were topically treated with 0.9% saline instilled to both eyes before UVB exposure (UVB group). The third group (three rabbits) served as controls (untreated animals).

The eye drops were administered by application of 50 µl of either drug or saline solution into the lower conjunctival fornix four times daily during 36 days. On day 37, all animals in the dxm/UVB and the UVB group were anaesthetised by i.m. injection of Rometar (Xylazinum hydrochloricum, 2%, Spofa, Czech Republic) (0.2 ml/kg body weight) and Narkamon (Ketaminum hydrochloricum, 5%, Spofa, CR) (1 ml/kg body weight) before exposure to UVB radiation. The eyes were open and the cornea was irradiated by UVB rays using an UVB lamp (Bioblock Scientific, Illkirch, France, wavelength 312 nm, 6 W) from a distance of 0.03 m for 10 minutes (the time of exposure), while the rest of the eye was protected. The intensity 3.2 mW/cm^2 (approx.) was achieved at this distance during the experiment. The total dose of irradiation was 2.05 J/cm^2. The intensity and dose were measured with a VLX – 3W Cole-Parmer Radiometer with microprocessor (Vernon Hills, Ill., USA) and Cole-Parmer UVB sensor (312 nm). Both eyes were treated in the same way. The lenses were examined with a hand-held slit-lamp during the treatment with steroids and immediately after the irradiation procedure. Twenty-four hours after the UVB exposure, the animals were sacrificed using thiopental anaesthesia and lens samples were prepared from each eye after enucleation (the lens sample from one eye in the dxm/UVB group was lost during preparation). The samples were immediately frozen and stored at –80°C prior to analysis by NMR spectroscopy. Animal experiments were performed in compliance with the "Principles of laboratory animal care" (NIH publication No. 85-23, revised 1985) and the OPRR Public Health Service Policy on the Humane Care and Use of Laboratory Animals.

NMR spectroscopy

The lenses were prepared for HR-MAS ^{1}H NMR spectroscopy. A cut was made along the lens axis (anterior-posterior), dividing the lens into two parts. A small meridional sector of one of the halves was obtained and weighed (20-40 mg), containing the whole radial profile with both cortical and nuclear parts of the lens. While still frozen, the lens sample was immersed in D_2O in a zirconium 4 mm 50 µl HR-MAS rotor. TSP (sodium-3'-trimethylsilylpropionate-2,2,3,3-d_4) was used as an internal shift reference substance (0 ppm). HR-MAS ^{1}H NMR spectroscopy was performed on a Bruker AVANCE DRX 600 spectrometer (14.1 T, Bruker BioSpin GmbH, Germany) equipped with a 4 mm HR-MAS ^{1}H/^{13}C probe. Samples were spun at 5000 Hz, temperature 4°C.

Proton spectra were obtained using a one-dimensional T_2-filtered sequence [$90° – (\tau – 180° – \tau)_n – acquisition$] (spin echo, CPMG – Carr-Purcell-Meiboom-Gill) [25, 29] to suppress signals from lipids and macromolecules. 512 transients were collected, using a 7.2 kHz spectral region with 32K data points. The T_2-filter contained delays of τ = 1 ms and n = 72 loops, giving an effective echo time of 144 ms. Acquisition time was 2.28 s, and zero-filling to 64K and an exponentially line broadening of 1 Hz was applied to the raw data before Fourier transformation. A selective presaturation pulse was applied to enhance the water suppression. Also, spectra were acquired using the NOESYPR1D pulse sequence [$relaxation\ delay – 90° – t_1 – 90° – t_m – 90° – acquisition$] (Bruker BioSpin GmbH), with t_1 fixed at 3 µs and a mixing time t_m of 100 ms. The water resonance was irradiated during the relaxation delay and t_m. The same spectral parameters and number of scans as in the T_2-filtered acquisitions were used.

For peak identification purposes, two-dimensional (2D) spectra such as magnitude-mode chemical shift correlated spectroscopy (COSY) and J-resolved spectra were acquired, all under MAS conditions. Gradient selected homonuclear COSY experiments were acquired with 64 transients, 256 time domain points in t_1, acquisition time 0.38 s and spectral width 5.4 kHz in both dimensions. The spectra were processed with unshifted sine window functions in both directions. HR-MAS ^{1}H NMR spectra were assigned with the aid of these 2D experiments and by comparison

with spectra of authentic compounds, together with reference to previous reports [7-9, 11, 14, 21, 26, 34, 37]. To analyse metabolic stability of the lens tissues during the HR-MAS NMR spectroscopy, some samples were spun continuously overnight at 4°C prior to a repeated acquisition. No obvious changes in lens metabolic profile were observed.

Statistical analysis

Both CPMG and NOESYPR1D HR-MAS NMR spectra were initially analysed by principal component analysis (The Unscrambler, CAMO, Norway). However, discrimination between treated and non-treated rabbit lenses was not different for the two types of spectra. Thus, further processing of the 1D spectra for the purpose of quantification was based on CPMG spectra, using software for analysis of complex mixtures (AMIX, Bruker BioSpin GmbH). The data were reduced to a resolution of 0.6 Hz/point, omitting the spectral region downfield from 5 ppm due to low signal-to-noise ratio. Metabolite concentrations in treated groups were calculated relative to the levels in the untreated group after normalisation (absolute NMR peak integrated/sample weight) [5]. Student's *t* test (two-tailed) was used for statistical analysis of the data. Statistical significance was set at $p < 0.05$ (confidence level at 95%).

Results

Representative T_2-filtered HR-MAS ^{1}H NMR spectra of the normal rabbit lens and lenses exposed to either only UVB radiation or combination of UVB and steroid pre-treatment are shown in Fig. 1. Signals from more than 15 major metabolites were assigned in the lens spectra, including glucose, reduced glutathione (GSH), sorbitol and sorbitol-3-phosphate, lactate, myo- and scyllo-inositol, glycine, taurine, glycerophosphocholine, phosphocholine, choline, glutamate, acetate, alanine and valine. Treatment with steroids in combination with UVB exposure induced more evident changes in the spectra than did only UVB irradiation. Compared to normal rabbit lens, substantial changes were observed in the spectral region 3.2 - 4.7 ppm of the lens treated with dexamethasone in combination with UVB. The most obvious was the decline of the β-amino acid taurine after this treatment (Fig. 1c). As shown in Fig. 1, intense signals from taurine were present in normal (1a) and UVB treated lenses (1b), represented with two triplets centred at chemical shifts (δ) 3.26 and 3.42 ppm, respectively. The results did not reveal significant difference in taurine concentration between normal and UVB treated lenses. However, after the combined treatment with steroids and UVB radiation, the signals from taurine were almost invisible (Fig. 1c).

As evident in Fig. 1, both the normal spectrum and the spectrum of UVB exposed lens were to a large extent dominated by signals from inositols in the shift range 3.2 - 4.1 ppm. In addition, this sugar/polyol region had signals from sorbitol and sorbitol-3-phosphate. Myo-inositol had a triplet at 3.27 ppm, neighbouring a triplet from taurine and singlets from choline containing compounds (choline, phosphocholine and glycerophosphocholine) in the crowded region 3.20 - 3.30 ppm. A double doublet at 3.54 and triplets at 3.62 and 4.06 ppm were assigned as myo-inositol. Scyllo-inositol was represented with a singlet at 3.35 ppm. Similar to taurine, the signals from myo- and scyllo-inositol were markedly depressed in the dxm/UVB group. Concomitantly, numerous peaks from glucose indicated an evident increase in its concentration after steroid/UVB treatment, while glucose signals were undetectable in the spectra of normal and only UVB exposed lens (Fig. 1). The accumulation of glucose and depletion of taurine and inositols is clearly demonstrated

in the two-dimensional COSY spectra in Fig. 2, presented as contour plots for the relevant spectral region. In the spectrum shown in Fig. 1c, the remaining small peaks of taurine in the dxm/UVB group were hidden under peaks arising from glucose. However, this residual amount of taurine could still be detected by two-dimensional spectroscopy (Fig. 2). Moreover, the dxm/UVB group showed an increase in signals from sorbitol and sorbitol-3-phosphate. In this group, the peaks in the spectral region 3.60 - 3.90 were mainly attributed to these two metabolites (Fig. 1c). In addition, the increased signal centred at 4.29 ppm was a multiplet assigned as sorbitol-3-phosphate.

Fig. 3 shows concentration levels of different metabolites in lenses exposed either to UVB radiation or a combination of UVB and steroid pre-treatment, expressed relative to the concentration in normal lenses. The extent of quantification was, however, limited in complex parts of the spectra with overlapping signals. Regarding observed differences between normal and UVB exposed lenses, the only significant changes ($p < 0.05$) were found for the concentration of glutamate and lactate. Thus, average concentration of glutamate in the lens increased by 40%, and lactate decreased by 35% after UVB exposure. Among the other metabolites showing a tendency to concentration change after UVB exposure, but without reaching a significant level, were increasing levels of alanine and the inositols, and a decrease of GSH level (Fig. 3).

Treatment with dexamethasone in combination with UVB exposure induced significant changes for several metabolites as compared to normal lens (Fig. 3). The concentration level of GSH was reduced by 54%, together with a substantial loss in inositol levels. The mean decrease in myo-inositol was 72%, equal to the mean reduction of scyllo-inositol. The concentration of lactate was reduced by 34%. Among the quantifiable amino acids, the level of alanine was more than doubled (107% increase) and the level of valine decreased by 28%. In addition, the level of choline decreased with 49% compared to the concentration in normal lens.

Despite all these metabolic changes measured with HR-MAS ^{1}H NMR spectroscopy in the lenses, all lenses remained clear as assured by regular slit-lamp examination of the rabbit eyes. No lens opacities could be detected by careful biomicroscopy one day after the UVB exposure.

Discussion

The results of this study show that UVB exposure alone or combined with steroid pre-treatment induced significant changes in the metabolic profile of rabbit lens. One of the striking effects of combined steroid and UVB treatment was the depletion of taurine. Taurine is the most abundant free amino acid in rabbit lens [19]. The rate of taurine uptake in the lens is very low, which implies the presence of an endogenous taurine-synthesising mechanism [30]. Taurine functions as an osmoregulator, ion flux regulator and membrane stabiliser [17]. In diabetic conditions taurine is depleted, which is considered the result of osmotic compensation in response to the accumulation of sorbitol within the lens [30]. Moreover, taurine is assumed to be active as an antioxidant. Reduced taurine in the lens might increase the risk of lens protein oxidation with subsequent cataract formation [24].

The combined treatment was also shown to cause a large reduction in the concentrations of inositols. Together with taurine and sorbitol, myo-inositol is one of the major osmolytes in the lens [46]. Using cultured bovine lens epithelial cells, Reeves and Cammarata [33] recognised the movement of myo-inositol from cell to medium, as induced by intracellular polyol accumulation. This polyol-activated myo-inositol release from the lens is a mechanism supporting our findings. Lowered myo-inositol and taurine levels following the combined treatment in our study suggest a change in osmotic regulation processes in the lens.

Lenses incubated with dexamethasone have shown a decrease in ATP concentration and an increase in sugar phosphates, suggesting that dexamethasone antagonised the cellular uptake or utilisation of glucose [13]. In the present study, the concentration level of lenticular glucose was shown to increase considerably following combined long-term steroid treatment/UVB radiation. Concomitantly, the concentration of lactate decreased reaching a level similar to that measured after UVB exposure only. In contrast, Pescosolido et al. [31] did not reveal any change in lenticular lactate concentration after long-term dexamethasone treatment of rabbit eyes. This implies that the decreased lactate concentration in our study possibly was caused by the UVB irradiation. Reduced lactate level might be due to inactivation of glycolytic enzymes after UVB exposure [22, 23, 35, 38].

A possible metabolic pathway of lenticular glucose is the conversion into sorbitol. In diabetic and galactosemic conditions, glucose is funneled into the polyol

pathway for conversion into sorbitol by activation of aldose reductase [18, 40]. Sugar alcohols poorly permeate cell membranes, so polyols accumulate intracellularly [24]. In diabetic lens, sorbitol-3-phosphate is produced from sorbitol by a 3-phosphokinase [20]. In the present study, sorbitol and sorbitol-3-phosphate were, on the basis of spectrum interpretation, found to increase after the combined treatment with steroids/UVB exposure. However, this was not exactly quantifiable due to severe spectral overlap. The decreased inositol and taurine levels, with a concomitant increase in sorbitol/sorbitol-3-phosphate, support previous reports [24, 31].

GSH is a vital lens antioxidant [10]. It is synthesised within the lens, and a common feature of most types of cataracts is a decrease in the GSH level [32]. It has been suggested that glucocorticoid activity mediated through a glucocorticoid receptor [15] is responsible for loss of lenticular GSH, and thereby leading to cataractogenesis [6]. In the present study, the concentration of GSH decreased considerably after the combined treatment. An accompanying increase in oxidised glutathione (GSSG) was not observed, which might indicate that GSH synthesis was impaired. In fact, GSSG was not detected in any lens from treated or untreated eyes. Under normal conditions, essentially all detectable cellular glutathione is in a reduced state [36]. Generally, HR-MAS ^{1}H NMR spectroscopy is an excellent method to discriminate between GSH and GSSG in unprocessed biological tissue.

The rise in alanine in both treated groups might be induced by the UVB radiation, as alanine is an oxidation product of tryptophan in the human lens [41].

As shown previously in studies with other biological tissues, HR-MAS ^{1}H NMR spectroscopy offers the ability to obtain high-resolution spectra from inhomogeneous samples with acceptable signal-to-noise ratio (S/N) [1, 4, 5, 28]. Due to its avascularity and the highly ordered state of its cells, the crystalline lens is a rewarding tissue for application of the MAS technique. To our knowledge, the present study has applied HR-MAS ^{1}H NMR spectroscopy in the analysis of lens tissue sections for the first time. The major advantage of the HR-MAS method is that high-quality spectra can be obtained from intact tissue samples. In contrast to previous reports on NMR spectroscopy of lens extracts from our laboratory and others [12, 26, 34], labour-intensive and tissue destructive extraction methods are avoided. Tissue extractions involve possible oxidation or hydrolysis of substances, and volatile compounds might be lost.

As compared to enzymatic and chromatographic methods, an inherent advantage of NMR spectroscopy is the simultaneous detection of different groups of compounds, e.g. amino acids and glycolytic intermediates and products. In addition, by means of the HR-MAS technique, water-soluble metabolites and lipids can be measured in the same sample.

Due to the non-destructive analysis in HR-MAS spectroscopy, also compartmentalisation of metabolites within different cellular environments can be assessed. Thus, HR-MAS NMR spectroscopy is a link to, and might be a step towards in vivo biochemical analysis of the lens by means of NMR spectroscopy.

In this study, frozen lens samples were sectioned and then put into the HR-MAS rotor. Efforts were made to keep the samples cooled until insertion into the spectrometer. During acquisition of spectra the temperature of the samples was kept at 4°C after careful calibration for heating effects due to spinning of the samples. As reported by Waters et al. [43], there might be some variation in the metabolic state of some tissues during MAS ^{1}H NMR experiments. Our study revealed a surprisingly high metabolic stability of lens samples during the analysis, a favourable finding for accomplishment of prolonged experiments with two-dimensional NMR spectroscopy.

Spectral quantification of the metabolites was based on CPMG spectra, i.e. filtered spectra in terms of T_2 relaxation. Hence, without accurate T_2 measurements, absolute quantification could not be performed. However, it was assumed that each metabolite has the same T_2 in different lenses, so a relative quantification was performed using absolute peak integrals normalised by sample weight.

The HR-MAS ^{1}H NMR spectra were acquired from a section of each lens. The standardised excised samples contained both cortical and nuclear parts, so spatially averaged metabolic profiles of the lenses were obtained. Minor inconsistencies during this procedure might however occur, providing lens samples with a larger inhomogeneity than desirable. Using this method, the metabolic asymmetry between nucleus, cortex and epithelium was not taken into account. For further work, an improved sectioning technique has been initiated to provide representative samples from either lens cortex or nucleus. Analysis of these regions separately would increase the benefit from HR-MAS NMR spectroscopy. Generally, spectra of good quality can be obtained from very small lenticular sections, making HR-MAS NMR

spectroscopy a potentially powerful tool for the study of disease or lenticular metabolic change due to drugs or endogenous pathophysiological stimuli.

In conclusion, HR-MAS ^{1}H NMR spectroscopy was found to be a valuable method for investigating the metabolic state of intact lens samples. The results show high-quality spectra with high signal-to-noise ratio from small lenticular sections. Significant metabolic changes were detected in the rabbit lens after long-term treatment with dexamethasone combined with a subsequent UVB exposure. The main findings include depletion of taurine and myo-inositol, an increase in glucose and sorbitols and a decrease in the GSH level. The metabolic state of the lens was changed more profoundly by long-term steroid treatment than by short-term UVB exposure. For the level of GSH, the effect of these two factors seems to be additive. The observed metabolic changes are in agreement with those reported by other studies and involved in the development of cataract.

Acknowledgements

Čestmír Čejka is gratefully acknowledged for radiometric measurements. This study was supported by grants from The Research Council of Norway, the grant from Grant Agency of Czech Republic No. 304/03/0419 and by the grant from the Academy of Sciences of the Czech Republic AVOZ5008914. JK thanks Bruker BioSpin, Rheinstetten, Germany, for continuous support in development of probes for making HR-MAS a viable method for metabolic profiling in tissue.

References

1. Bollard ME, Garrod S, Holmes E, Lindon JC, Humpfer E, Spraul M, Nicholson JK (2000) High-resolution ^{1}H and ^{1}H-^{13}C magic angle spinning NMR spectroscopy of rat liver. Magn Reson Med 44: 201-207
2. Bucala R, Gallati M, Manabe S, Cotlier E, Cerami A (1985) Glucocorticoid-lens protein adducts in experimentally induced steroid cataracts. Exp Eye Res 40: 853-863
3. Bucala R, Manabe S, Urban RC, Cerami A (1985) Nonenzymatic modification of lens crystallins by prednisolone induces sulfhydryl oxidation and aggregate formation: in vitro and in vivo studies. Exp Eye Res 41: 353-363
4. Cheng LL, Chang I-W, Smith BL, Gonzalez RG (1998) Evaluating human breast ductal carcinomas with high-resolution magic-angle spinning proton magnetic resonance spectroscopy. J Magn Reson 135: 194-202
5. Cheng LL, Lean CL, Bogdanova A, Wright SC Jr, Ackerman JL, Brady TJ, Garrido L (1996) Enhanced resolution of proton NMR spectra of malignant lymph nodes using magic-angle spinning. Magn Reson Med 36: 653-658
6. Dickerson JE Jr, Dotzel E, Clark AF (1997) Steroid-induced cataract: new perspectives from in vitro and lens culture studies. Exp Eye Res 65: 507-516
7. Fan TW-M (1996) Metabolite profiling by one- and two-dimensional NMR analysis of complex mixtures. Prog NMR Spectrosc 28: 161-219
8. Ferretti A, D'Ascenzo S, Knijn A, Iorio E, Dolo V, Pavan A, Podo F (2002) Detection of polyol accumulation in a new ovarian carcinoma cell line, CABA I: a ^{1}H NMR study. Br J Cancer 86: 1180-1187
9. Garrod S, Humpher E, Connor SC, Connelly JC, Spraul M, Nicholson JK, Holmes E (2001) High-resolution ^{1}H NMR and magic angle spinning NMR spectroscopic investigation of the biochemical effects of 2-bromoethanamine in intact renal and hepatic tissue. Magn Reson Med 45: 781-790
10. Giblin FJ (2000) Glutathione: a vital lens antioxidant. J Ocul Pharmacol Ther 16: 121-135
11. Govindaraju V, Young K, Maudsley AA (2000) Proton NMR chemical shifts and coupling constants for brain metabolites. NMR Biomed 13: 129-153

12. Greiner JV, Auerbach DB, Leahy CD, Glonek T (1994) Distribution of membrane phospholipids in the crystalline lens. Invest Ophthalmol Vis Sci 35: 3739-3746
13. Greiner JV, Kopp SJ, Glonek T (1982) Dynamic changes in the organophosphate profile upon treatment of the crystalline lens with dexamethasone. Invest Ophthalmol Vis Sci 23: 14-22
14. Gribbestad IS, Petersen SB, Fjøsne HE, Kvinnsland S, Krane J (1994) ^{1}H NMR spectroscopic characterization of perchloric acid extracts from breast carcinomas and non-involved breast tissue. NMR Biomed 7: 181-194
15. Gupta V, Wagner BJ (2003) Expression of the functional glucocorticoid receptor in mouse and human lens epithelial cells. Invest Ophthalmol Vis Sci 44: 2041-2046
16. Hightower K, McCready J (1992) Physiological effects of UVB irradiation on cultured rabbit lens. Invest Ophthalmol Vis Sci 33: 1783-1787
17. Huxtable RJ (1989) Taurine in the central nervous system and the mammalian actions of taurine. Prog Neurobiol 32: 471-533
18. Kador PF, Akagi Y, Kinoshita JH (1986) The effect of aldose reductase and its inhibition on sugar cataract formation. Metabolism 35: 15-19
19. Kinsey VE (1965) Amino acid transport in the lens. Invest Ophthalmol 4: 691-699
20. Lal S, Szwergold BS, Taylor AH, Randall WC, Kappler F, Wells-Knecht K, Baynes JW, Brown TR (1995) Metabolism of fructose-3-phosphate in the diabetic rat lens. Arch Biochem Biophys 318: 191-199
21. Lindon JC, Nicholson JK, Everett JR (1999) NMR spectroscopy of biofluids. In: Webb GA (ed) Annual Reports on NMR Spectroscopy, vol 38. Academic Press, London, pp 1-88
22. Löfgren S, Söderberg PG (1995) Rat lens glycolysis after in vivo exposure to narrow band UV or blue light radiation. J Photochem Photobiol B 30: 145-151
23. Löfgren S, Söderberg PG (2001) Lens lactate dehydrogenase inactivation after UV-B irradiation: An in vivo measure of UVR-B penetration. Invest Ophthalmol Vis Sci 42: 1833-1836
24. Malone JI, Lowitt S, Cook WR (1990) Nonosmotic diabetic cataracts. Pediatr Res 27: 293-296

25. Meiboom S, Gill D (1958) Modified spin-echo method for measuring nuclear relaxation times. Rev Sci Instrum 29: 688-691
26. Midelfart A, Dybdahl A, Gribbestad IS (1996) Detection of different metabolites in the rabbit lens by high resolution ^{1}H NMR spectroscopy. Curr Eye Res 15: 1175-1181
27. Midelfart A, Dybdahl A, Krane J (1999) Detection of dexamethasone in the cornea and lens by NMR spectroscopy. Graefes Arch Clin Exp Ophthalmol 237: 415-423
28. Moka D, Vorreuther R, Schicha H, Spraul M, Humpfer E, Lipinski M, Foxall PJD, Nicholson JK, Lindon JC (1997) Magic angle spinning proton nuclear magnetic resonance spectroscopic analysis of intact kidney tissue samples. Anal Comm 34: 107-109
29. Nicholson JK, Foxall PJD, Spraul M, Farrant RD, Lindon JC (1995) 750 MHz ^{1}H and ^{1}H-^{13}C NMR spectroscopy of human blood plasma. Anal Chem 67: 793-811
30. Obrosova IG, Stevens MJ (1999) Effect of dietary taurine supplementation on GSH and NAD(P)-redox status, lipid peroxidation, and energy metabolism in diabetic precataractous lens. Invest Ophthalmol Vis Sci 40: 680-688
31. Pescosolido N, Miccheli A, Manetti C, Iannetti GD, Feher J, Cavallotti C (2001) Metabolic changes in rabbit lens induced by treatment with dexamethasone. Ophthalmic Res 74: 68-74
32. Reddy VN (1990) Glutathione and its function in the lens - an overview. Exp Eye Res 50: 771-778
33. Reeves RE, Cammarata PR (1996) Osmoregulatory alterations in myo-inositol uptake by bovine lens epithelial cells. Part 5: Mechanism of the myo-inositol efflux pathway. Invest Ophthalmol Vis Sci 37: 619-629
34. Risa Ø, Sæther O, Midelfart A, Krane J, Čejková J (2002) Analysis of immediate changes of water-soluble metabolites in alkali-burned rabbit cornea, aqueous humor and lens by high-resolution ^{1}H-NMR spectroscopy. Graefes Arch Clin Exp Ophthalmol 240: 49-55
35. Schmidt J, Schmitt C, Kojima M, Hockwin O (1992) Biochemical and morphological changes in rat lenses after long-term UV B irradiation. Ophthalmic Res 24: 317-325
36. Spector A, Huang R-R, Wang G-M (1985) The effect of H_2O_2 on lens epithelial cell glutathione. Curr Eye Res 4: 1289-1295

37. Szwergold BS, Kappler F, Brown TR, Pfeffer P, Osman SF (1989) Identification of D-sorbitol 3-phosphate in the normal and diabetic mammalian lens. J Biol Chem 264: 9278-9282
38. Tung WH, Chylack LT Jr, Andley UP (1988) Lens hexokinase deactivation by near-UV irradiation. Curr Eye Res 7: 257-263
39. Urban RC Jr, Cotlier E (1986) Corticosteroid-induced cataracts. Surv Ophthalmol 31: 102-110
40. van Heyningen R (1959) Formation of polyols by the lens of the rat with "sugar" cataract. Nature 184: 194-195
41. van Heyningen R (1975) What happens to the human lens in cataract. Sci Am 233: 70-81
42. Watanabe H, Kosano H, Nishigori H (2000) Steroid-induced short term diabetes in chick embryo: Reversible effects of insulin on metabolic changes and cataract formation. Invest Ophthalmol Vis Sci 41: 1846-1852
43. Waters NJ, Garrod S, Farrant RD, Haselden JN, Connor SC, Connelly J, Lindon JC, Holmes E, Nicholson JK (2000) High-resolution magic angle spinning ^{1}H NMR spectroscopy of intact liver and kidney: optimization of sample preparation procedures and biochemical stability of tissue during spectral acquisition. Anal Biochem 282: 16-23
44. Wegener A, Hockwin O (1987) Animal models as a tool to detect the subliminal cocataractogenic potential of drugs. Concepts Toxicol 4: 250-262
45. West SK, Valmadrid CT (1995) Epidemiology of risk factors for age-related cataract. Surv Ophthalmol 39: 323-334
46. Yokoyama T, Lin L-R, Chakrapani B, Reddy VN (1993) Hypertonic stress increases NaK ATPase, taurine, and myoinositol in human lens and retinal pigment epithelial cultures. Invest Ophthalmol Vis Sci 34: 2512-2517

Figure legends

Fig. 1 HR-MAS ^{1}H NMR spectra of rabbit lenses. a) Normal lens, b) lens after UVB exposure and c) lens treated with dexamethasone in combination with UVB exposure. Assignments: Glc, glucose; GSH, reduced glutathione; Sorb, sorbitol; Sorb-3-P, sorbitol-3-phosphate; Lac, lactate; M-ins, myo-inositol; S-ins, scyllo-inositol; Gly, glycine; Tau, taurine; GPC, glycerophosphocholine; PC, phosphocholine; Cho, choline; Glu, glutamate; Ace, acetate; Ala, alanine; Val, valine.

Fig. 2 Two-dimensional ^{1}H COSY contour plots (3.14-3.52 ppm) of rabbit lens treated with dexamethasone in combination with UVB exposure (left) and untreated lens (right). Corresponding one-dimensional T_2-filtered spectra are shown above (all spectra obtained under MAS conditions). Abbreviations as in Fig. 1.

Fig. 3 Changes in metabolite concentrations in rabbit lens after UVB exposure (n = 6) and after treatment with dexamethasone (dxm) in combination with UVB exposure (n = 7), measured as % change (± 95% C.I.) compared to concentrations in the normal lens (n = 6). For abbreviations, cf. Fig. 1.

Figure 1

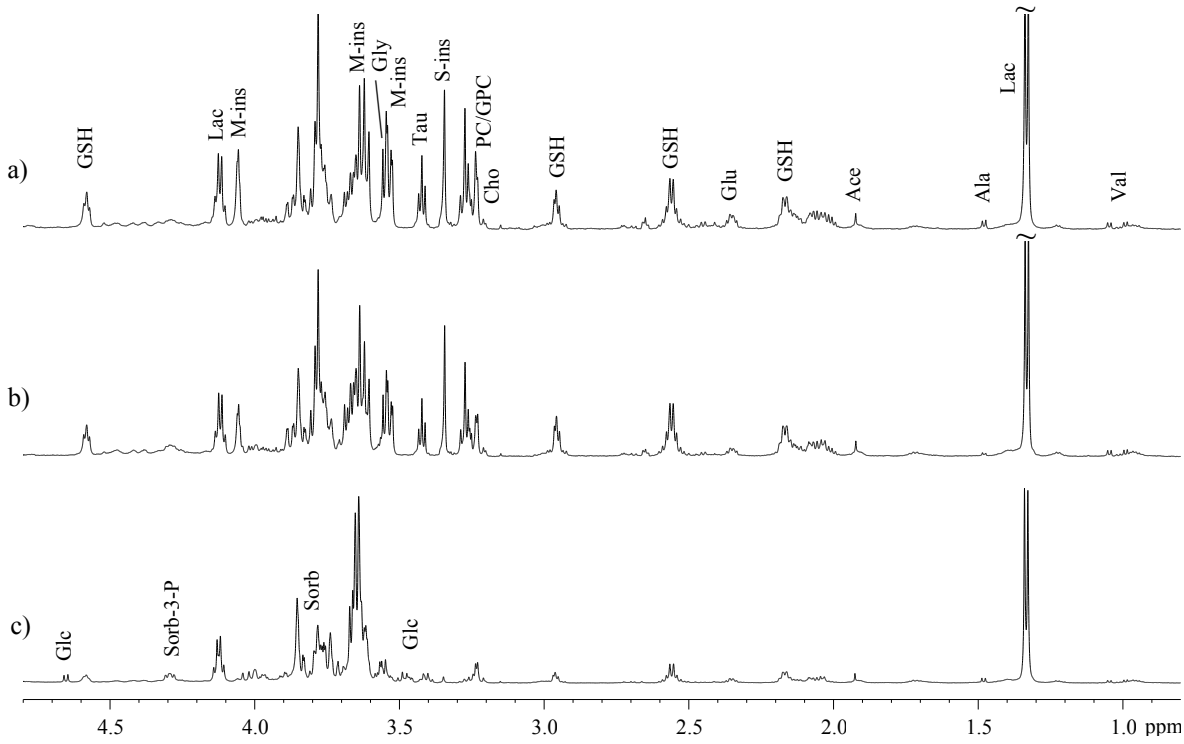
a)
b)
c)
GSH
Lac
M-ins
M-ins
Gly
M-ins
Tau
S-ins
PC/GPC
Cho
GSH
GSH
Glu
GSH
Ace
Ala
Lac
Val
Glc
Sorb-3-P
Sorb
Glc
4.5
4.0
3.5
3.0
2.5
2.0
1.5
1.0 ppm

Figure 2

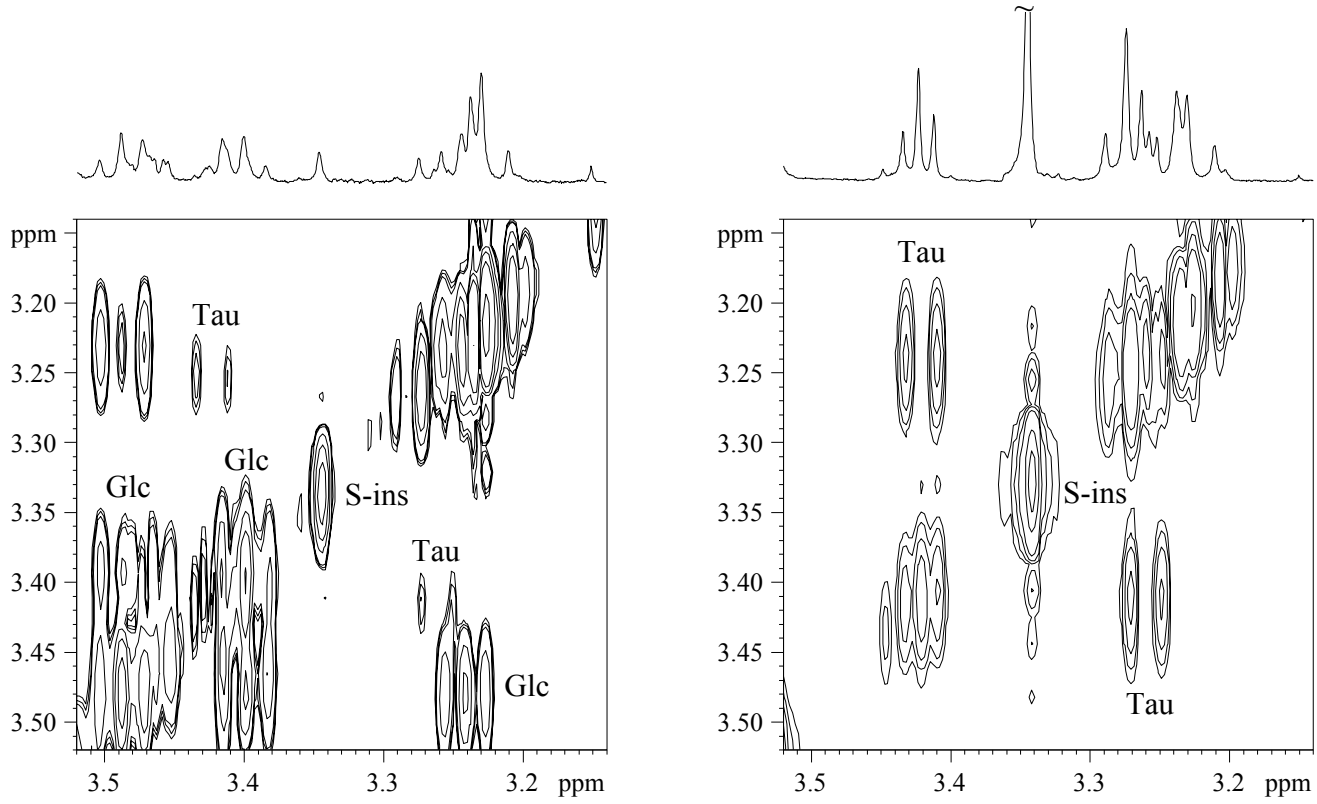
ppm
3.20
3.25
3.30
3.35
3.40
3.45
3.50
Tau
Glc
Glc
S-ins
Tau
Glc
3.5
3.4
3.3
3.2
ppm
ppm
3.20
3.25
3.30
3.35
3.40
3.45
3.50
Tau
S-ins
Tau
3.5
3.4
3.3
3.2
ppm

Figure 3

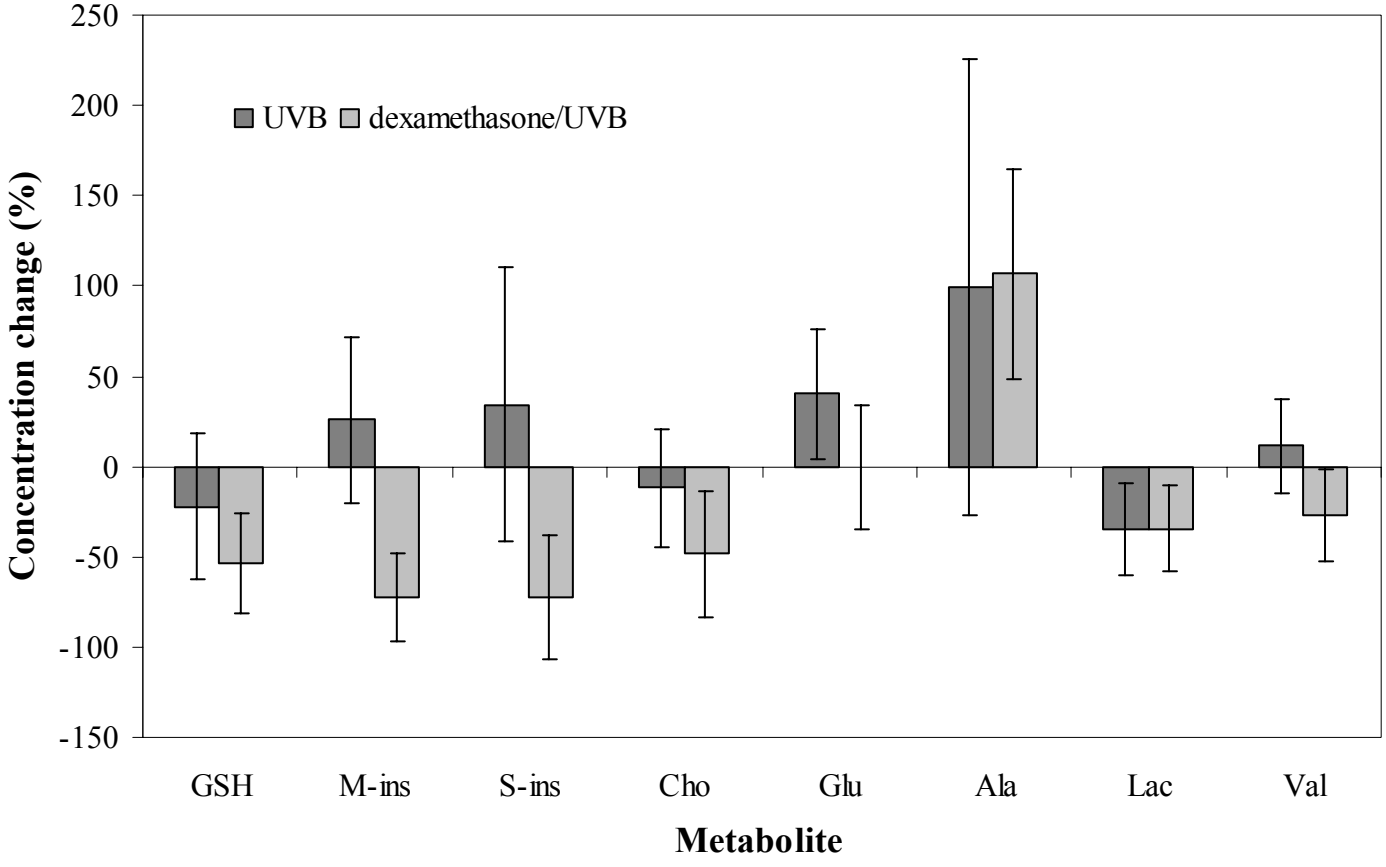
250
200
150
100
50
0
-50
-100
-150
UVB
dexamethasone/UVB
Concentration change (%)
GSH
M-ins
S-ins
Cho
Glu
Ala
Lac
Val
Metabolite